JINR grant
(#6, Flow and Global characteristics of collisions) intermediate report

A. Taranenko, M. Mamaev, I. Segal, V. Troshin, D. Idrisov,
P. Parfenov, A. Demanov

Main topics of the grant:

1. Service work for the MPD collaboration in terms of supporting and further improving existing methods for determining centrality based on Glauber Monte Carlo and Inverse Bayes methods. Development of a common framework for centrality determination (TPC+FHCAL).

1. Analysis of collective flow using fully reconstructed model data for the Bi+Bi system at an energy of 9.2 GeV in the center of mass frame. Verification and validation of the new versions of heavy-ion collision models.

1. Development, maintenance, support and documentation of the software for the collective flow analysis in the MPD experiment, using both two- and many-particle methods. Further development of the universal QnTools package.

Reports in the MPD Cross-PWG in 2023 related to the grant

- 17.01: D. Idrisov “Centrality determination sensitivity to multiplicity cuts”
- 14.02: V. Troshin “FFD and FHCal comparison for flow analysis in the MPD experiment”
- 14.02: I. Segal “Centrality determination with Monte-Carlo sampling procedure for spectators energy”
- 28.03: D. Idrisov “Correlation between mean transverse momentum and anisotropic flow in models at NICA energy range”
- 11.07: A. Demanov “Elliptic and triangular flow for identified hadrons from the vHLLE+UrQMD for BiBi@9.2 GeV (Request 32)”
- 05.09: M. Mamaev “Performance study of the anisotropic flow measurements with fixed-target mode of the MPD experiment at NICA”
- 19.09: D. Idrisov “Centrality determination method in nuclear collisions by using hadron calorimeter”
- 19.09 A. Taranenko JINR grant (#6, flow and global characteristics of collisions) intermediate report1

Reports on the conferences and other events/Publications in 2023

- **INFINUM-2023 (23.02-03.03):**
  - A. Taranenko “What we can learn from particle flow in HICs?”
  - P. Parfenov “The heavy-ion program at the upgraded Baryonic Matter@Nuclotron Experiment at NICA”
- **LomCon-2023 (24-30.08):**
  - I. Segal “Mehods for centrality determination in heavy-ion collisions with the BM@N experiment”
  - P. Parfenov “Anisotropic flow and its scaling properties at Nuclotron-NICA energies”
  - V. Troshin “Performance of FFD detector for anisotropic flow analysis with the MPD experiment”
  - M. Mamaev “On the proton directed and elliptic flow in the few-GeV heavy ion collisions with BM@N”
- **ISHEPP-2023 (18-23.09):**
  - A. Taranenko “Anisotropic collective flow measurements from LHC to SIS”
  - A. Demanov “Elliptic flow fluctuations at NICA energy range”
  - P. Parfenov “Performance study of the anisotropic flow measurements of identified charged hadrons with fixed-target mode of the MPD experiment at NICA “
  - M. Mamaev “Directed and elliptic flow of protons in the heavy ion collisions at 2-4 GeV”
  - I. Segal “Methods for centrality determination in heavy-ion collisions based on Monte-Carlo sampling of spectator fragments “
  - **NICA Days 2023, XII MPD Collaboration meeting (2-7.10,2023)**

    A. Taranenko Collective Flow in Heavy-Ion Collisions

    P. Parfenov , PWG3 Summary

Publications: A special issue of Particles (ISSN 2571-712X). - 5 publications
https://www.mdpi.com/journal/particles/special_issues/physics_performance

Main topic 1: Centrality determination in the MPD experiment using spectator energy for MC-Glauber and inverse Bayes methods

Motivation for centrality determination

- Evolution of matter produced in heavy-ion collisions depends on its initial geometry

- **Goal of centrality determination**:
  map (on average) the collision geometry parameters
  to experimental observables (centrality estimators)

- Centrality class S_1-S_2: group of events corresponding to a given fraction (in %) of the total cross section:

$$C_S = \frac{1}{\sigma_{inel}^{AA}} \int_{S_1}^{S_2} \frac{d\sigma}{dS} dS$$

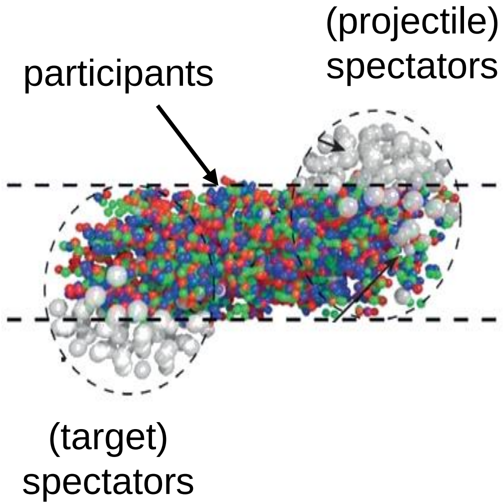

Centrality determination based on Monte-Carlo sampling

For **multiplicity of produced particles** used in HADES, CBM, BM@N, NA61/SHINE

Get (N_{part}, N_{coll}) from MC-Glauber

Calculate $N_a = fN_{part} + (1-f)N_{coll}$

Sample multiplicity of produced particles (S_i) N_a times from NBD (μ, k)

For **any spectators based observable** used in CBM, BM@N

For **spectators energy** from hadron calorimeters used in NA61/SHINE

Get (N_{spec}, b) from MC-Glauber

Calculate (A_{tot}) - at t=∞

Sample (A_{frag},N_{Afrag}) for (A_{tot}, N_{spec}, b)

Sample (E_{frag},y_{frag}) for (A_{frag})

Sample S_{frag} for (E_{frag},y_{frag})

Sample hadron calorimeter response (S_i) N_{spec} times from Gauss(μ, k)

Result: total S_{tot}

MC-Glauber distribution

Full Monte-Carlo (real data) distribution

Evaluate χ^2 between $dN/dE_{MC/data}$ and dN/dE_{Gl}

Scan phase space of parameters to find their values for minimum of χ^2

Extract relation between geometry parameters and centrality estimator

Simplified MC sampling for hadron calorimeters

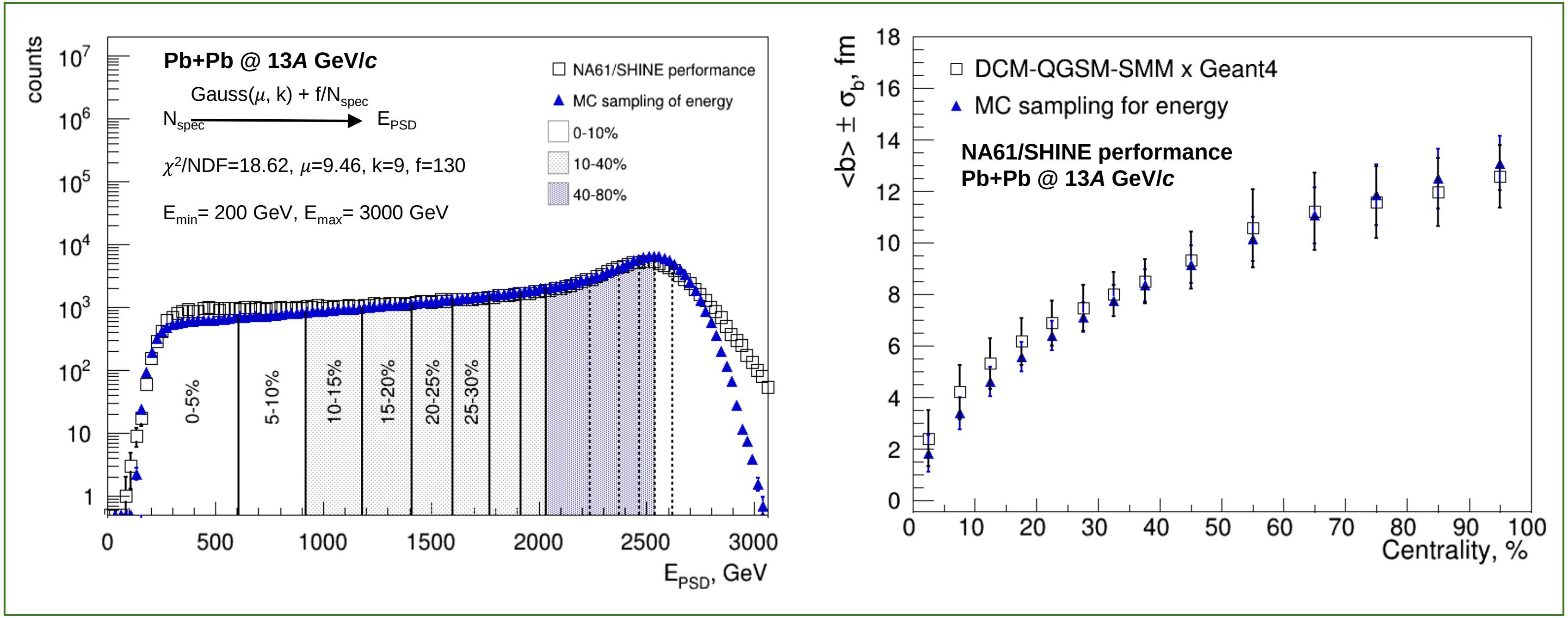

- Simplified procedure for spectators energy is tested on NA61 data
- Gauss distribution can not reproduce energy distribution in the most central collisions
- Possible improvements are now under investigation

The Bayesian inversion method (Γ-fit): main assumptions

Relation between multiplicity N_{ch} and impact parameter b

is defined by the fluctuation kernel:

$$P(E \mid c_b) = \frac{1}{\Gamma(k(c_b))\theta^2} E^{k(c_b)-1} e^{-E/\theta}$$

$$\theta = \frac{D(E)}{\langle E \rangle}, \quad k = \frac{\langle E \rangle}{\theta}$$

$c_b = \int_0^b P(b')db'$ – centrality based on impact parameter

$\langle E \rangle, \quad D(E)$ – average value and variance of energy

$$\langle E \rangle = \mu_1 \langle E'(c_b) \rangle + \lambda_1, \quad D(E) = \mu_2 D(E'(c_b))$$

Three fit parameters μ_1, μ_2, λ_1

$\langle E'(c_b) \rangle, \quad D(E'(c_b))$ – average value and variance of energy from the model

These quantities can be approximated by polynomials

$$\langle E'(c_b) \rangle = \sum_{j=1}^{8} a_j c_b^j, \quad D(E'(c_b)) = \sum_{j=1}^{6} b_j c_b^j$$

2 main steps of the method:

Fit experimental (model) distribution with P(E)

↓

Construct P(b|E) using Bayes' theorem: P(b|E) = P(b)P(E|b)/P(E)

Comparison with MC-Glauber fit

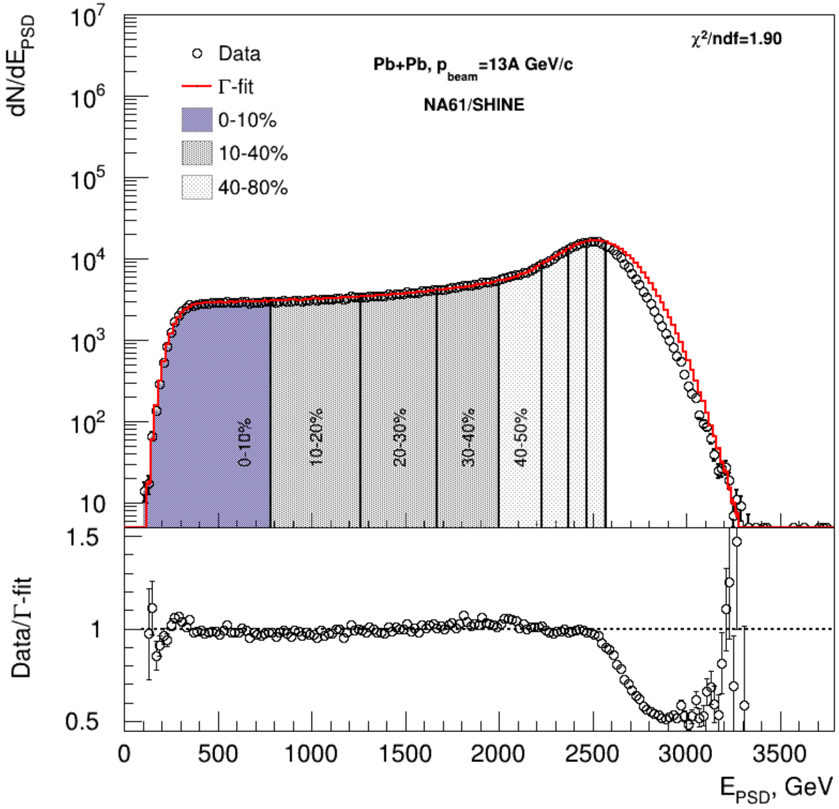

Good agreement between fit and data.

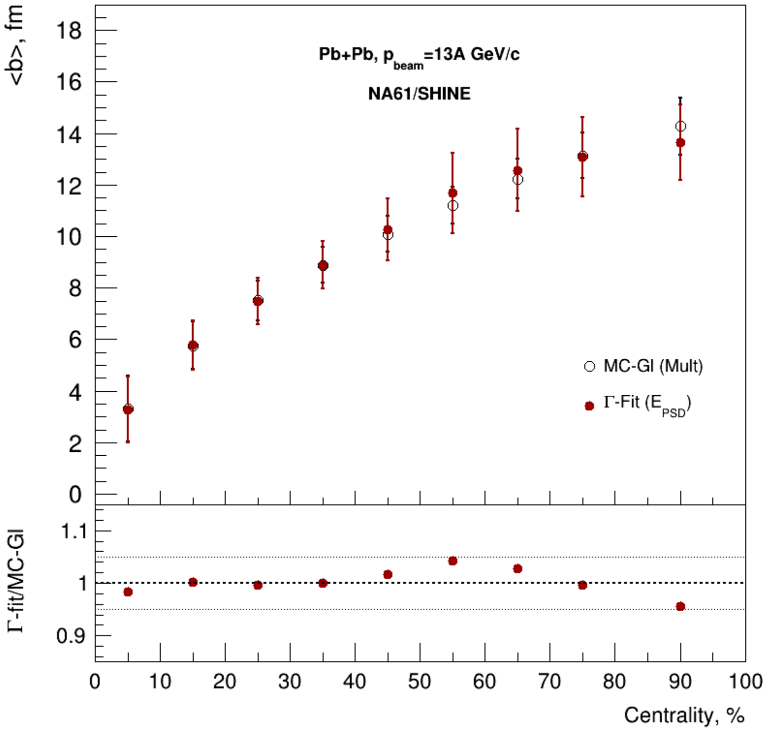

There is agreement within 5%.

Summary for main topic 1

- Software implementation of MC Glauber and Γ-fit with multiplicity based fitting procedure is used for MPD
- Relation between impact parameter and centrality classes is extracted

- Centrality determination procedures based on MC sampling of spectators energy are developed and tested based on NA61/SHINE data for both MC-Glauber and inverse Bayes approaches
- Results are tuned on the spectator production implemented in the DCM-QGSM-SMM model
- Simplified procedure for hadron calorimeters based on Gauss distribution is also proposed for MC-Glauber approach

Work in progress

- Investigate the effect on centrality determination due to the fragment loss in beam hole of the MPD FHCal
- Introduce detailed parametrization for steps of centrality determination procedure and improve current parametrization
- Apply this procedure for MPD FHCal simulations

Main topic 2: Performance for anisotropic flow measurements using UrQMD model (req. 25) for the second collaboration paper

Methods for v_n measurements

- **Sub-event 2-particle Q-cumulants v2{2}:** Δη=0.1 is applied between 2 sub-events A, B to suppress non-flow

$$Q_n = \sum_{i=1}^{M} e^{in\phi} \qquad \langle 2 \rangle_{a|b} = \frac{Q_{n_a} Q^*_{n,b}}{M_a M_b} \qquad v_2\{2\} = \sqrt{\langle\langle 2 \rangle\rangle_{a|b}}$$

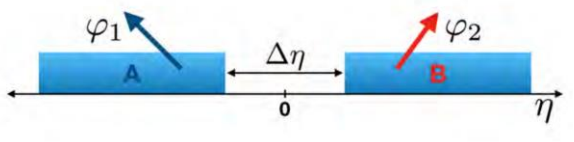

- **4-particle Q-cumulants v2{4}**

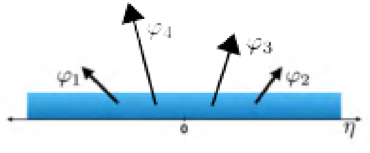

$$\langle 2 \rangle = \frac{|Q_n|^2 - M}{M(M-1)}$$

$$v_2\{4\} = \sqrt[4]{2\,\langle\langle 2 \rangle\rangle^2 - \langle\langle 4 \rangle\rangle}$$

$$\langle 4 \rangle = \frac{|Q_n|^4 + |Q_{2n}|^2 - 2\Re[Q_{2n} Q^*_n Q^*_n] - 4(M-2)\,|Q_n|^2 - 2M(M-3)}{M(M-1)(M-2)(M-3)}$$

- **Event plane method:** Δη=0.1

$$Q_{n,x} = \sum_i w_i \cos(n\phi_i)$$
$$Q_{n,y} = \sum_i w_i \sin(n\phi_i)$$

$$\Psi_n^{EP} = \frac{1}{n}\tan^{-1}\left(\frac{Q_{n,y}}{Q_{n,x}}\right)$$

$$v_n = \frac{\langle \cos[n(\phi - \Psi_n^{EP})] \rangle}{\sqrt{\langle \cos\,[n(\Psi_{n,a} - \Psi_{n,b})] \rangle}}$$

Here: $\boldsymbol{\omega_i}$ - $p_{T,i}$ transverse momentum of the i-th track in the TPC

$\boldsymbol{\varphi_i}$ - azimuthal angle of the i-th track in the TPC

Ψ_n- event plane angles

Method’s details described in PRC 83 (2011), 044913 , EP method: Phys.Rev.C 77 (2008) 034904

Performance of v_1 (pT,y) measurements

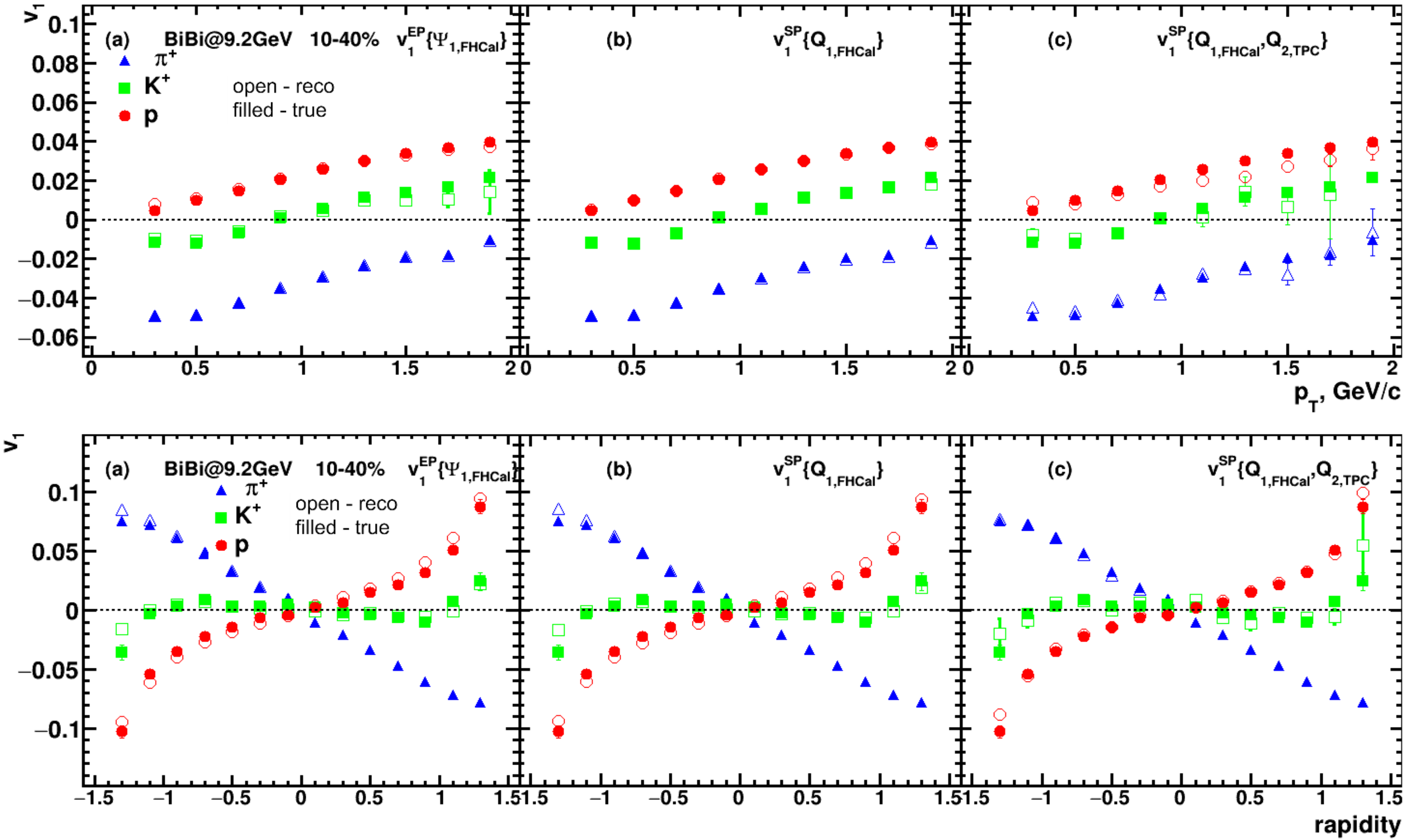

Performance of v_2(pT) measurements

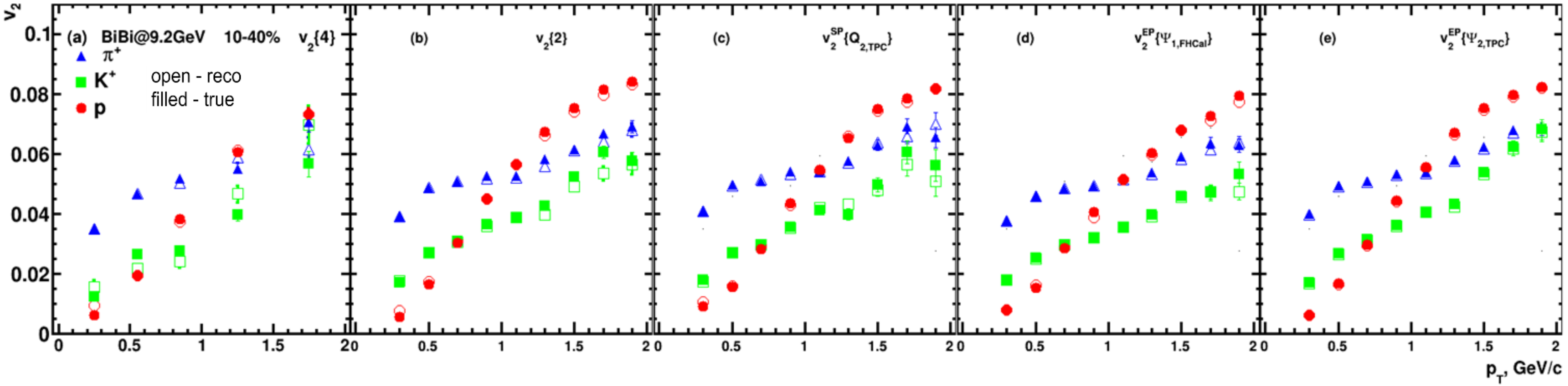

Results using reconstructed tracks (reco) are consistent with results obtained from MC particles (true) for both v_1, v_2 and all used methods (EP, SP, Q-Cumulants)

Main topic 2: Anisotropic flow measurements using vHLLE+UrQMD hybrid model (req. 32)

Event plane Resolution

2 sub event: Δη=0.1

$$Res\{\Psi_n^{E(W)}\} = \sqrt{\langle \cos\left[n(\Psi_n^E - \Psi_n^W)\right]\rangle}$$

Anisotropic flow is measured as follows:

$$v_n = \frac{\langle \cos[n(\phi - \Psi_n^{EP})]\rangle}{\sqrt{\langle \cos\left[n(\Psi_{n,a} - \Psi_{n,b})\right]\rangle}}$$

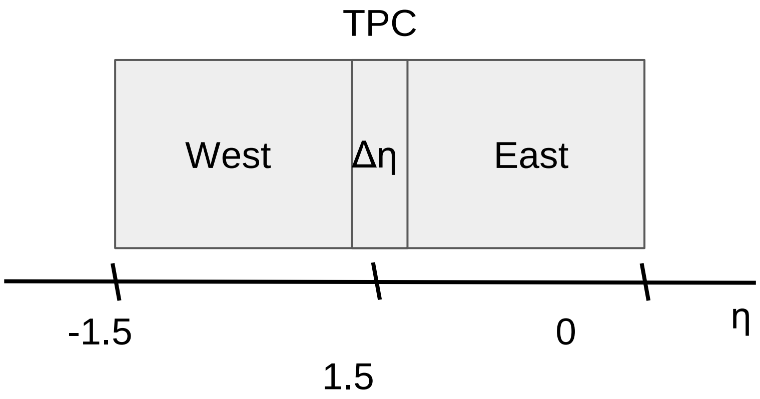

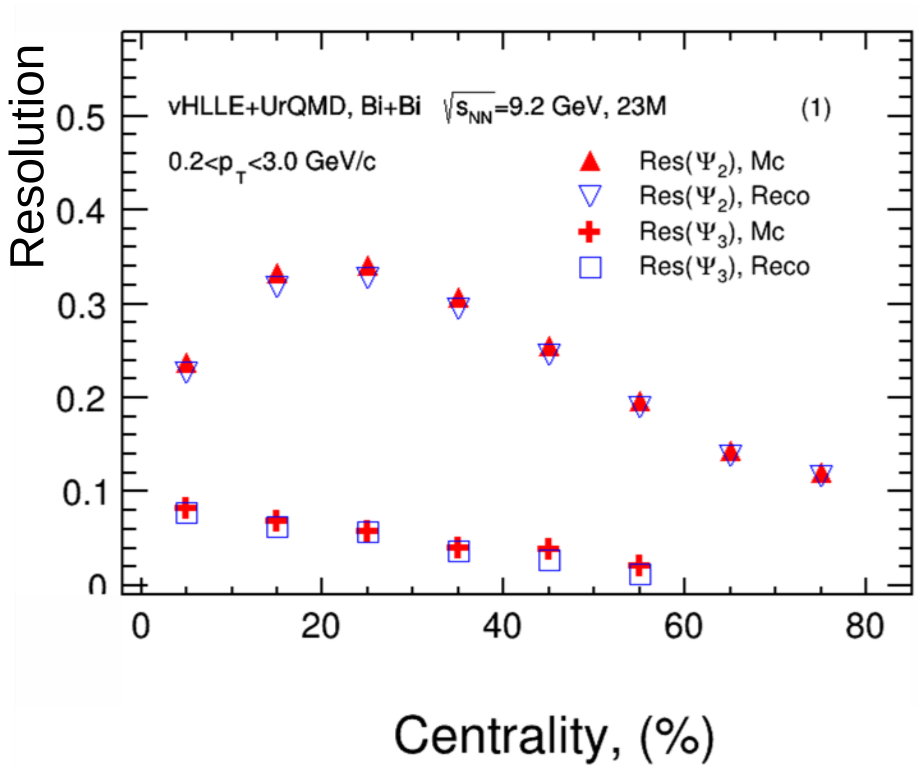

- We do not measure the Ψ_3 resolution after to 60% centrality
- Ψ_3 resolution are smaller than Ψ_2
- Good agreement between $R_{MC}(\Psi_n)$ and $R_{reco}(\Psi_n)$

Comparison of Reco and MC: v_2 eta-sub EP

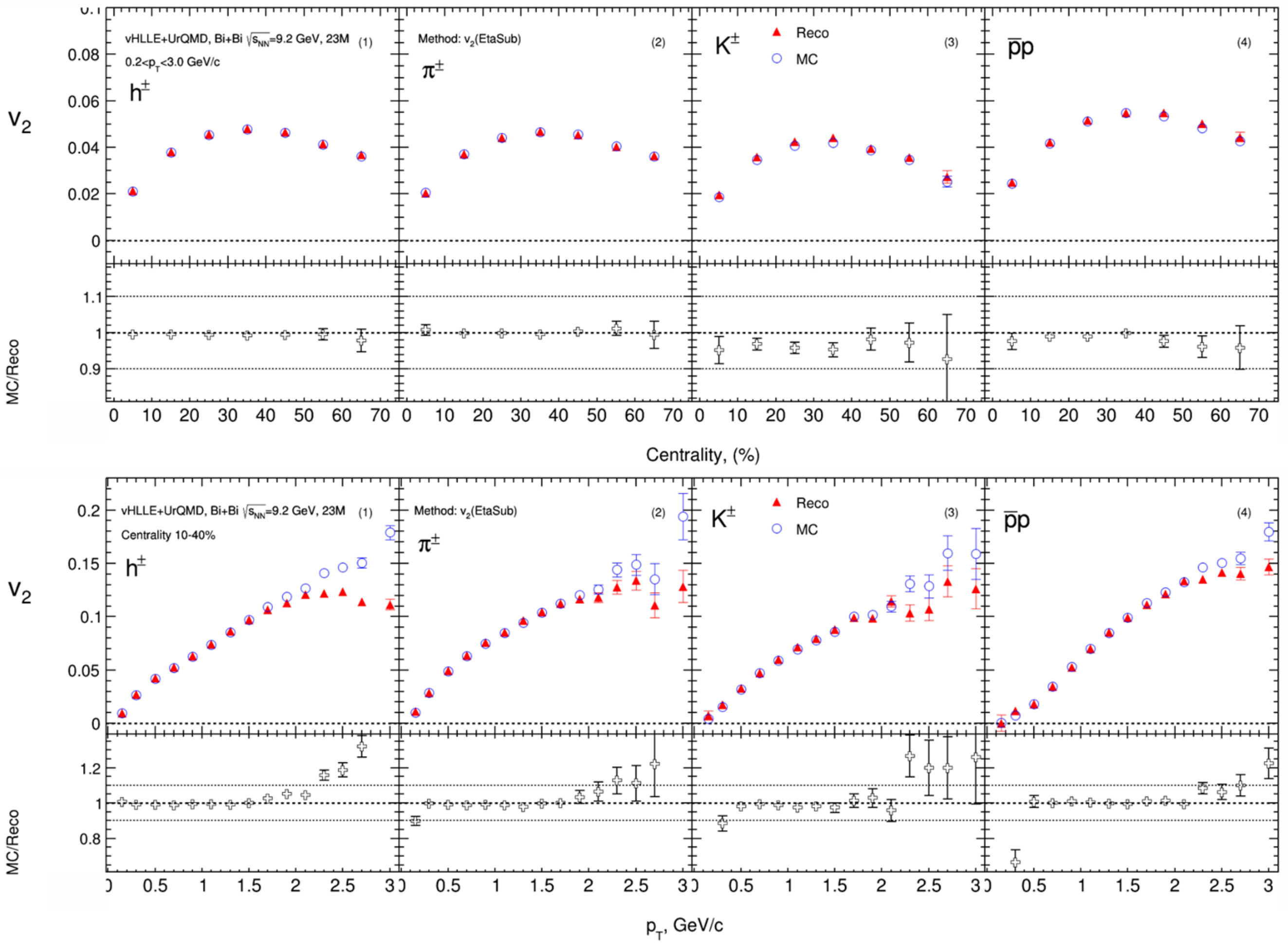

Cuts:

- Charged particles only
- Primary
- $|\eta|<1.5$
- $\Delta\eta = 0{,}1$
- $p_T > 0.2$ GeV/c
- $|DCA|<3\sigma$
- nTPC hits ≥ 16
- PID: PDG code

❑ good agreement of the $v_{2,mc}$ with $v_{2,reco}$ data

❑ The difference at large p_T between $v_{2,mc}$ and $v_{2,reco}$ (non-flow?)

Comparison of Reco and MC: v_2 eta-sub EP

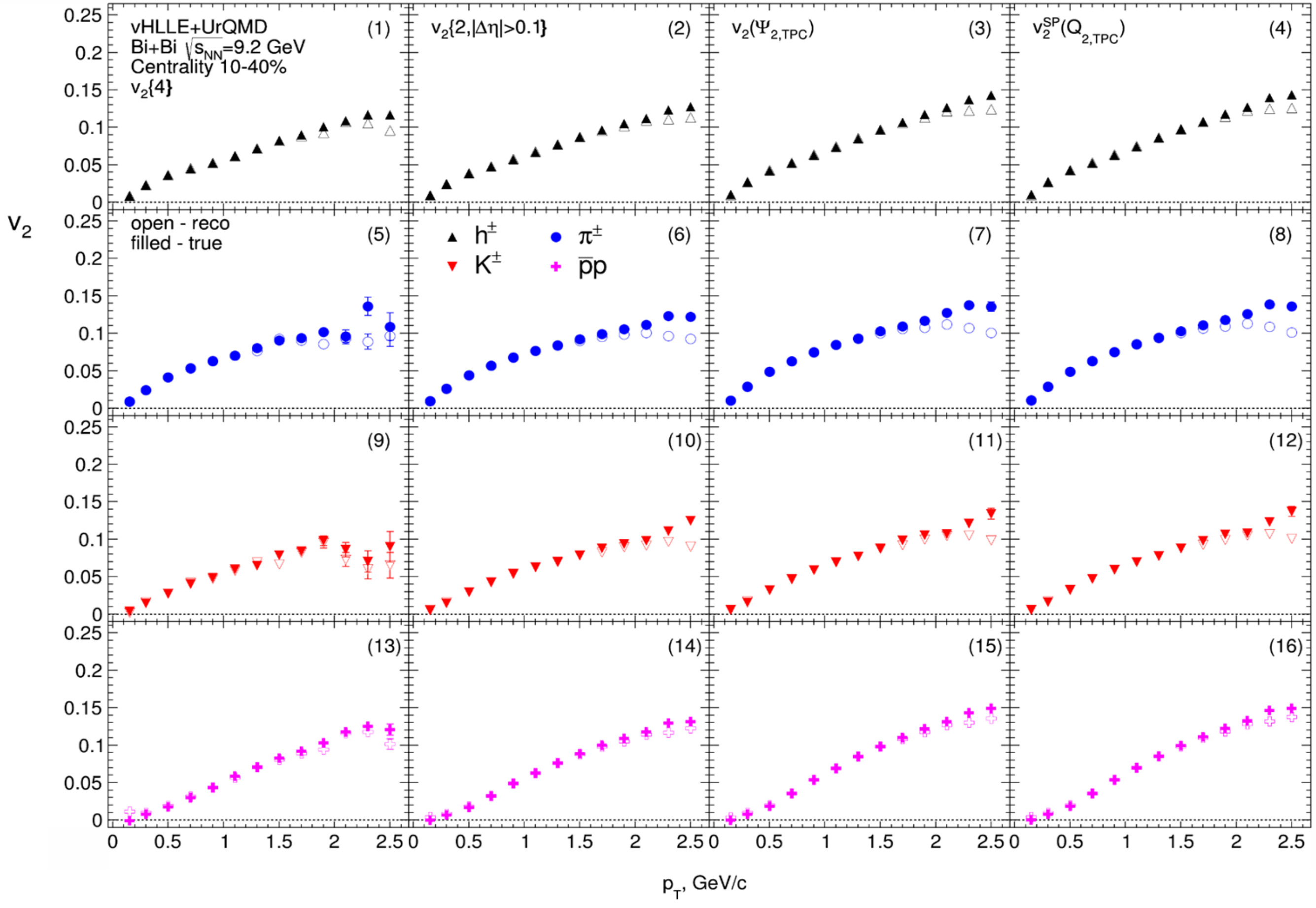

Cuts:

- Charged particles only
- Primary
- $|\eta|<1.5$
- $\Delta\ \eta = 0{,}1$
- $p_T > 0.2$ GeV/c
- $|DCA|<3\sigma$
- nTPC hits ≥ 16
- PID: PDG code

- good agreement of the $v_{2,mc}$ with $v_{2,reco}$ data
- The difference at highp_T between $v_{2,mc}$ and $v_{2,reco}$ (non-flow)

Comparison of Reco and MC: v_3 eta-sub EP

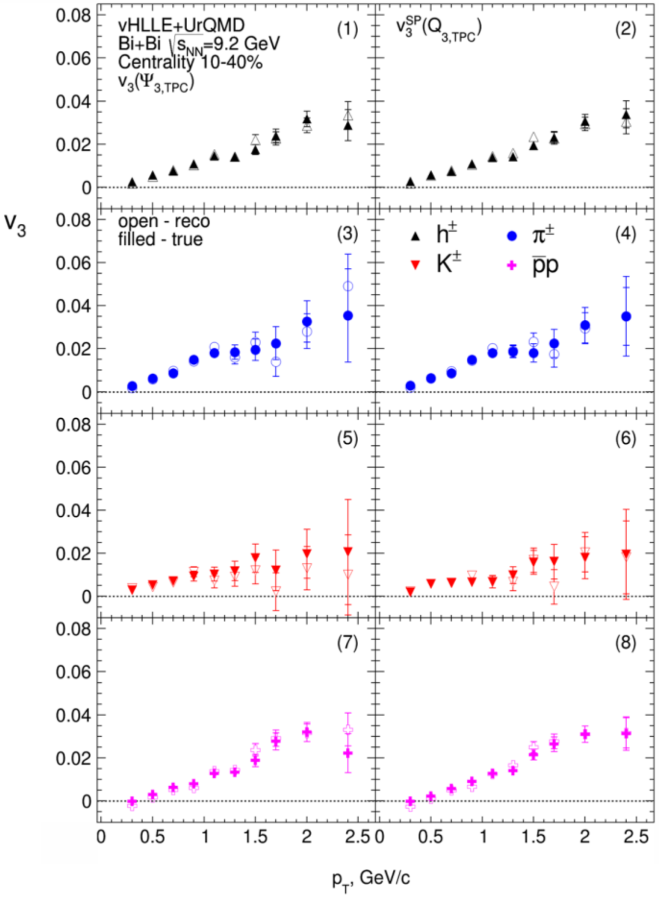

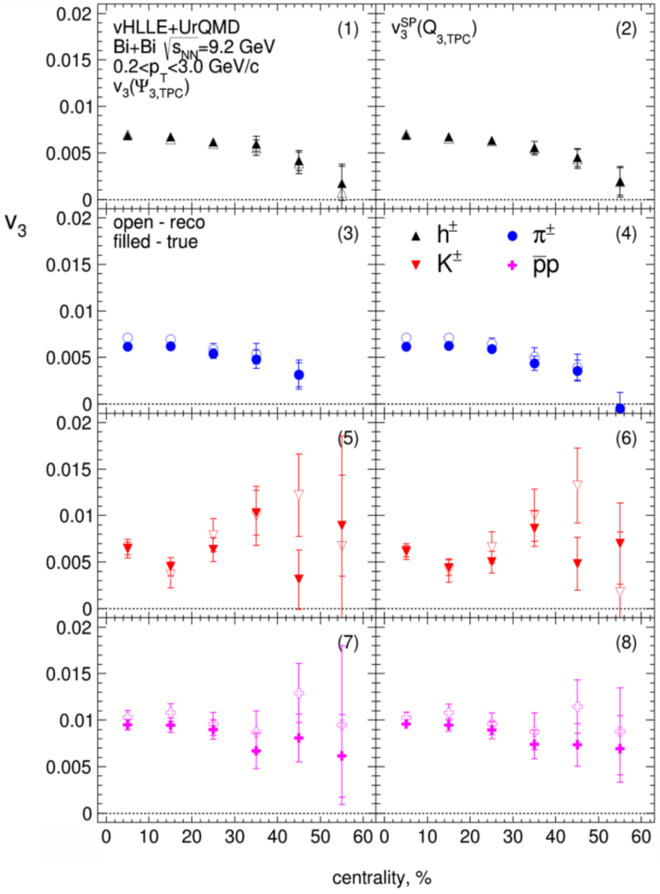

Cuts:

- Charged particles only
- Primary
- $|\eta|<1.5$
- $\Delta\eta = 0{,}1$
- $p_T > 0.2$ GeV/c
- $|DCA|<3\sigma$
- nTPC hits ≥ 16
- PID: PDG code

- ❑ Good performance for v_3 measurements
- ❑ More statistics needed for more precise v_3 measurements

Summary for main topic 2

- **Flow measurements for UrQMD model (req. 25):**
    - Directed and elliptic flow measurements were done using several methods: event plane, scalar product and Q-Cumulant.
    - Results are ready for the second collaboration paper
- **Flow measurements for vHLLE+UrQMD model (req. 32):**
    - Observed outlier events in the distribution Mult vs b - typical for this model
    - Centrality classes have been determined using the Inverse Bayes method. For this model, flow measurements (without cut on Mult vs b) are possible up to 50-60%
    - There is a good agreement between $v_{2,mc}$ and $v_{2,reco}$. But there are differences at large p_T region - contribution from non-flow.

evPlane wagon for EP measurements in MPD

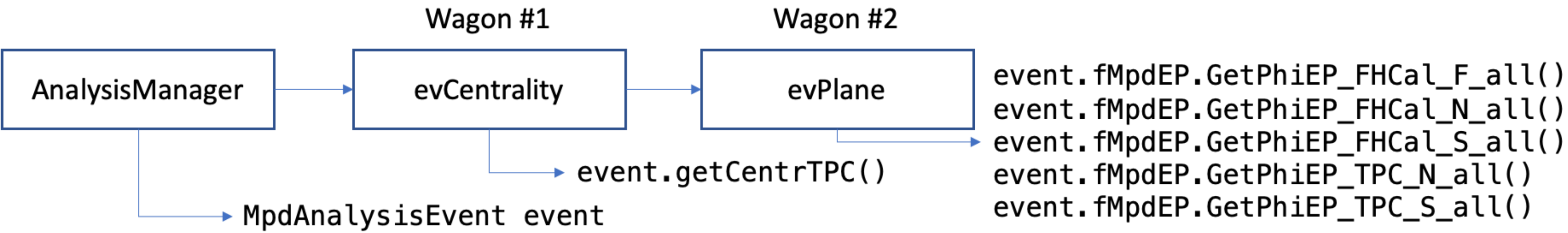

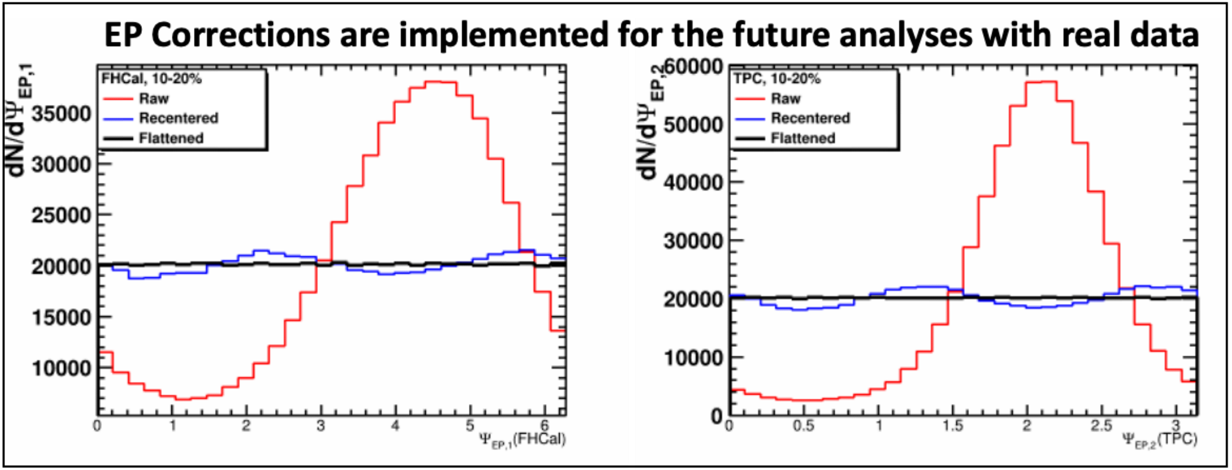

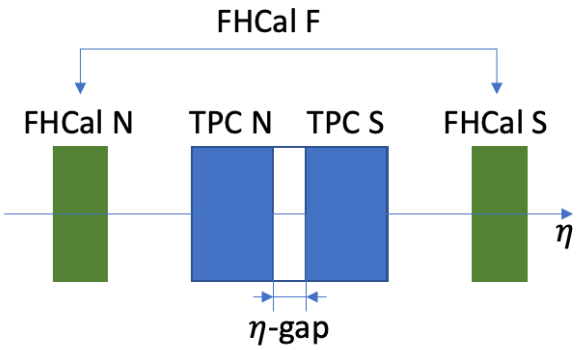

- **evPlane wagon is implemented into MPD Analysis Framework and is already being used in the collaboration**
- **Wagon for the flow measurements (Event Plane method) is on its way**

Main topic 3: Performance of the FFD detector in anisotropic flow measurements

FHCal and FFD detectors

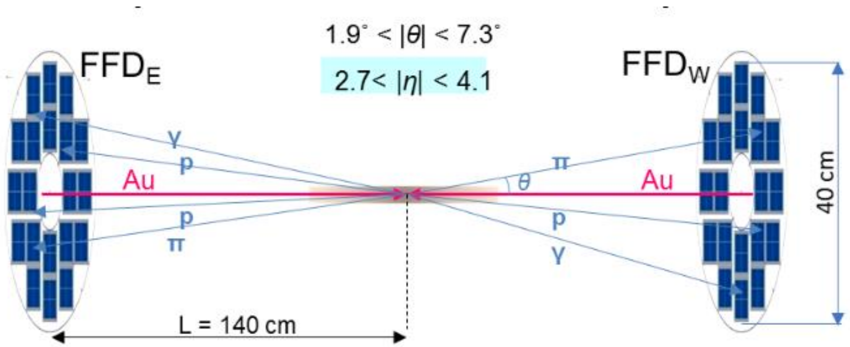

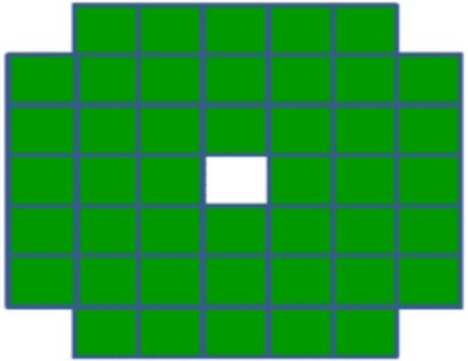

The FFD consists of two sets of Cherenkov counters located at ±140 cm from the nominal interaction point. Each set has 20 physical detectors with 4 read-out channels each. As a result, the total number of read-out channels is 2 sides 80 channels = 160 channels.

FHCal consists of two sets of hadron calorimeters in pseudorapidity region $2<|\eta|<5$ Each set has 44 modules form azimuthal symmetry. Total number of modules 88.

Directed flow of charged hadrons with FHCal and FFD

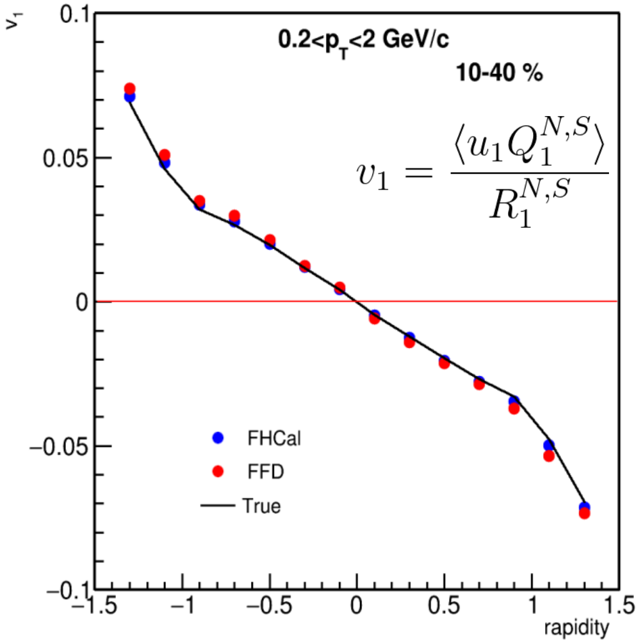

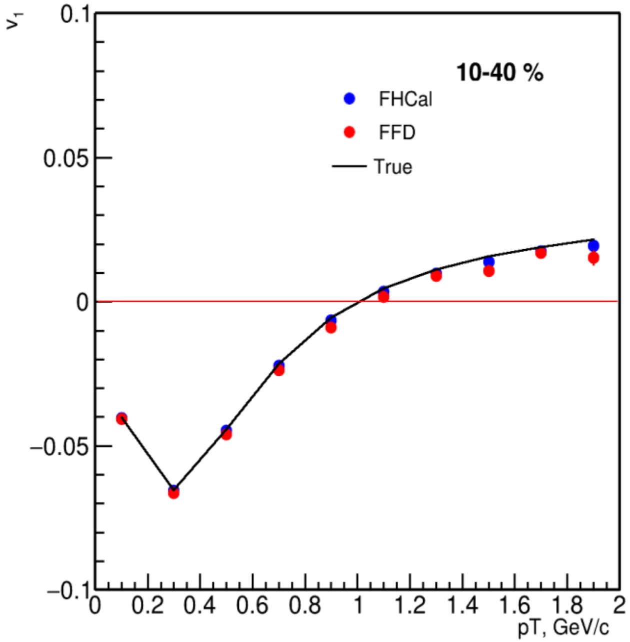

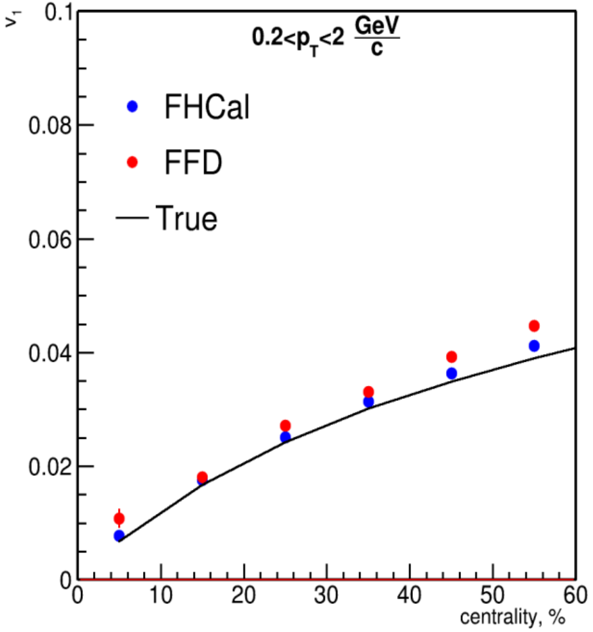

FHCal and FFD have consistent results; both can be used for directed flow measurements.

Elliptic flow of charged hadrons with FHCal and FFD

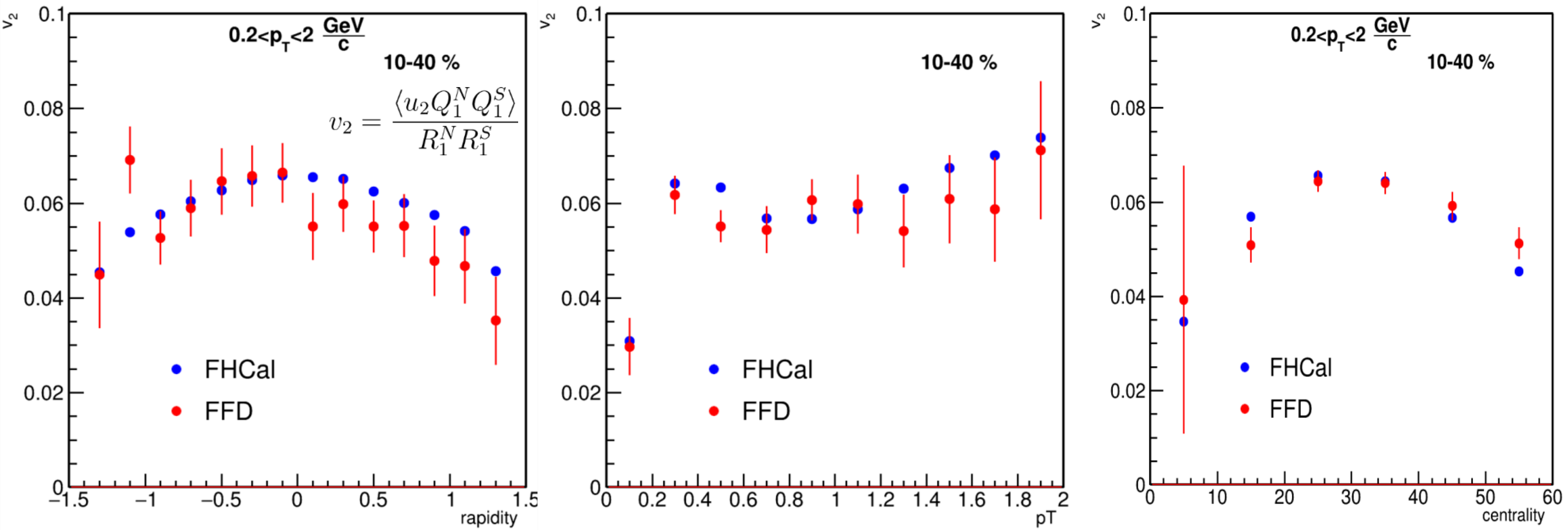

Due to low Resolution FFD need more statistics than FHCal for elliptic flow measurements.

Main topic 3: Performance study for the anisotropic flow measurements in the MPD experiment with the fixed-target mode (MPD FXT)

Flow performance study for MPD in fixed-target mode

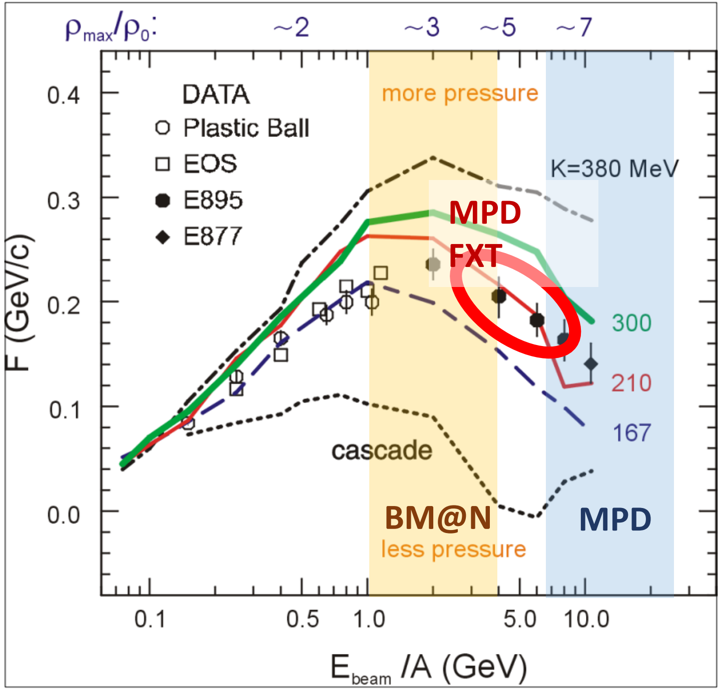

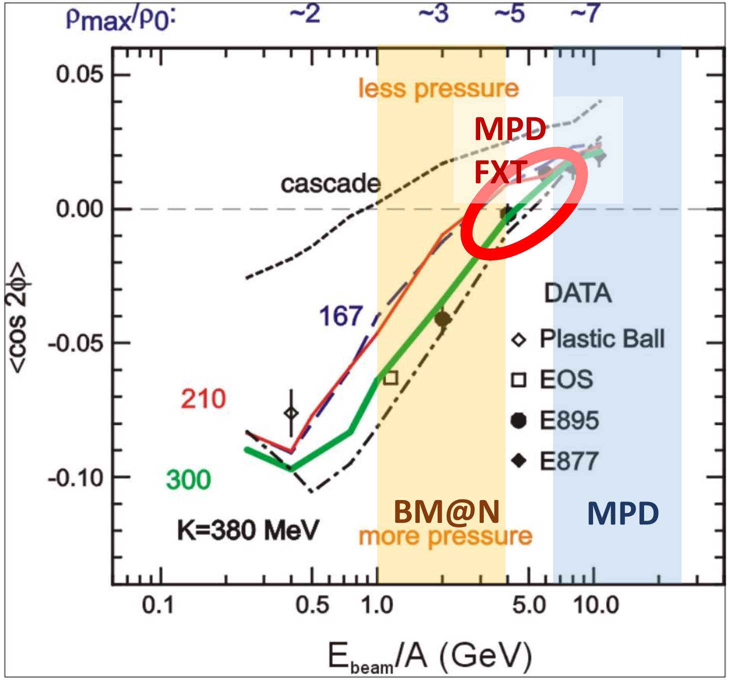

P. DANIELEWICZ, R. LACEY, W. LYNCH
10.1126/science.1078070

- **The flow data from E895 experiment have ambiguous interpretation:**
  v_1 suggests soft EOS while v_2 corresponds to hard EOS
- **Additional measurements are essential to clarify the previous measurements**

MPD in Fixed-Target Mode (FXT)

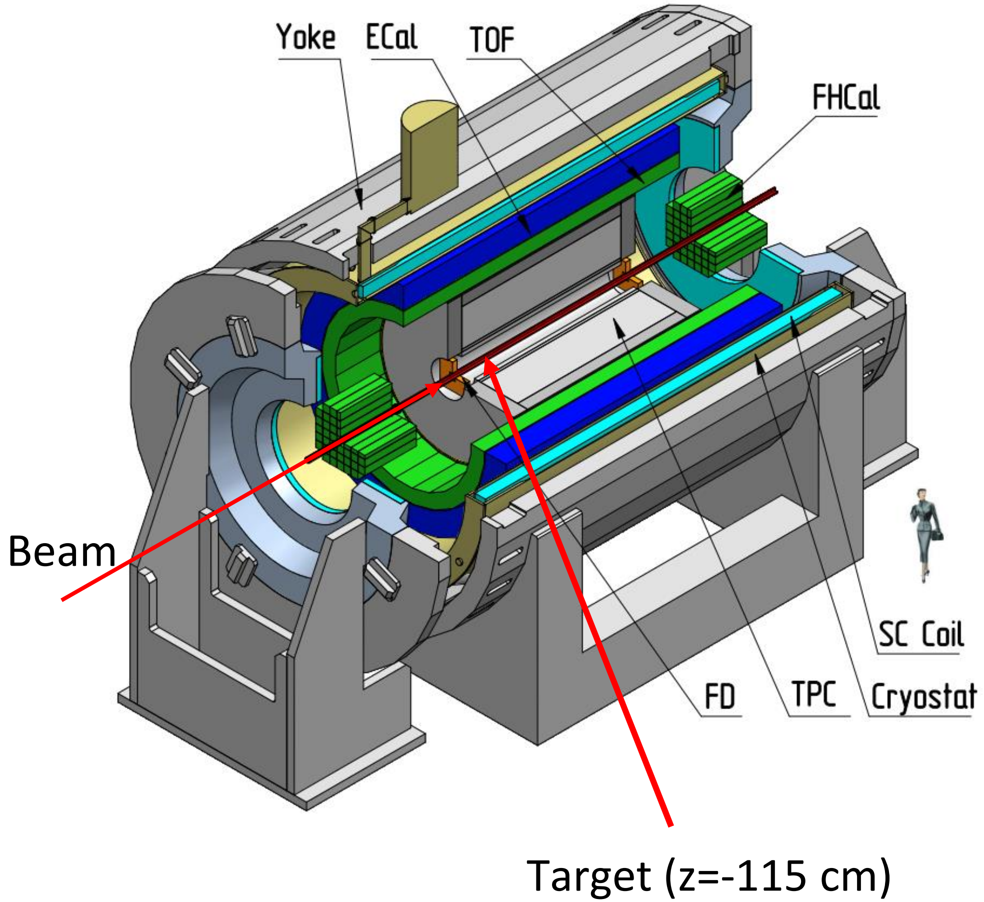

- Model used: UrQMD mean-field
  - Bi+Bi, E_{kin}=1.45 AGeV ($\sqrt{s_{NN}}$=2.5 GeV)
  - Bi+Bi, E_{kin}=2.92 AGeV ($\sqrt{s_{NN}}$=3.0 GeV)
  - Bi+Bi, E_{kin}=4.65 AGeV ($\sqrt{s_{NN}}$=3.5 GeV)
- Point-like target
- GEANT4 transport
- Particle species selection via true-PDG code of the associated MC particle

Flow vectors

From momentum of each measured particle define a u_n-vector in transverse plane:

$$u_n = e^{in\phi}$$

where φ is the azimuthal angle

Sum over a group of u_n-vectors in one event forms Q_n-vector:

$$Q_n = \frac{\sum_{k=1}^{N} w_n^k u_n^k}{\sum_{k=1}^{N} w_n^k} = |Q_n| e^{in\Psi_n^{EP}}$$

Ψ_n^{EP} is the event plane angle

Modules of FHCal divided into 3 groups

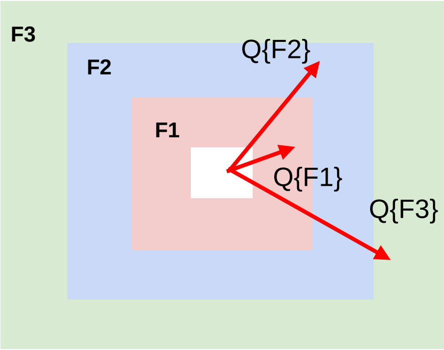

π-   p

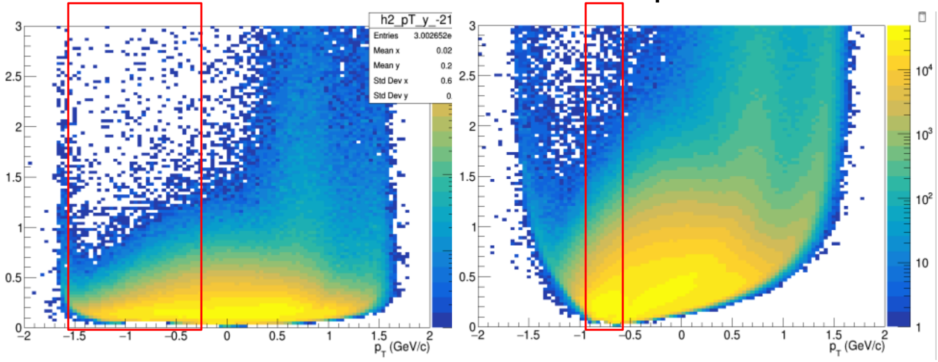

Additional subevents from tracks not pointing at FHCal:

Tp: p; -1.0<y<-0.6;

Tπ: π-; -1.5<y<-0.2;

MPD-FXT: v_1 for protons

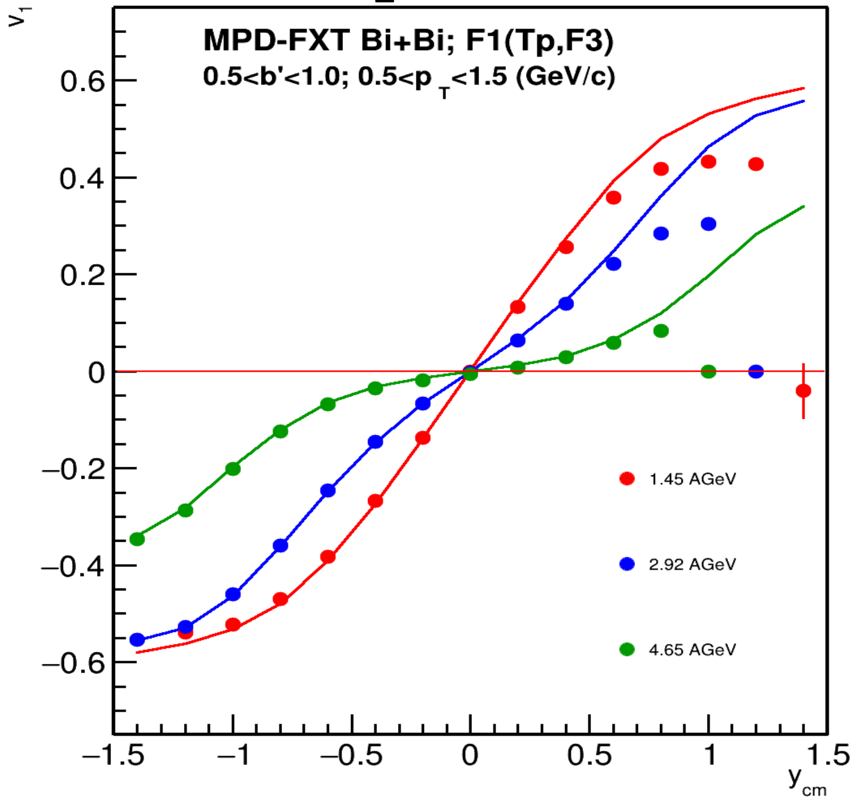

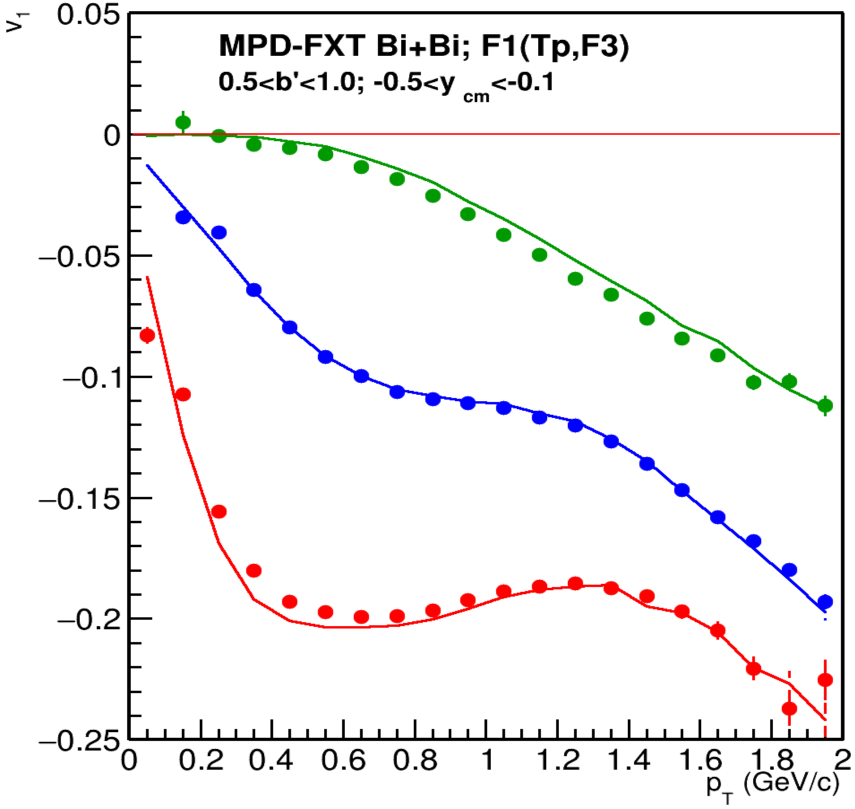

v_1 is consistent with model signal for y < 0.5

No efficiency corrections were applied yet

BM@N vs MPD: v_1 vs y for protons

See M.Mamaev's talk at ISHEP-2023
and at Cross-PWG 5.09.2023

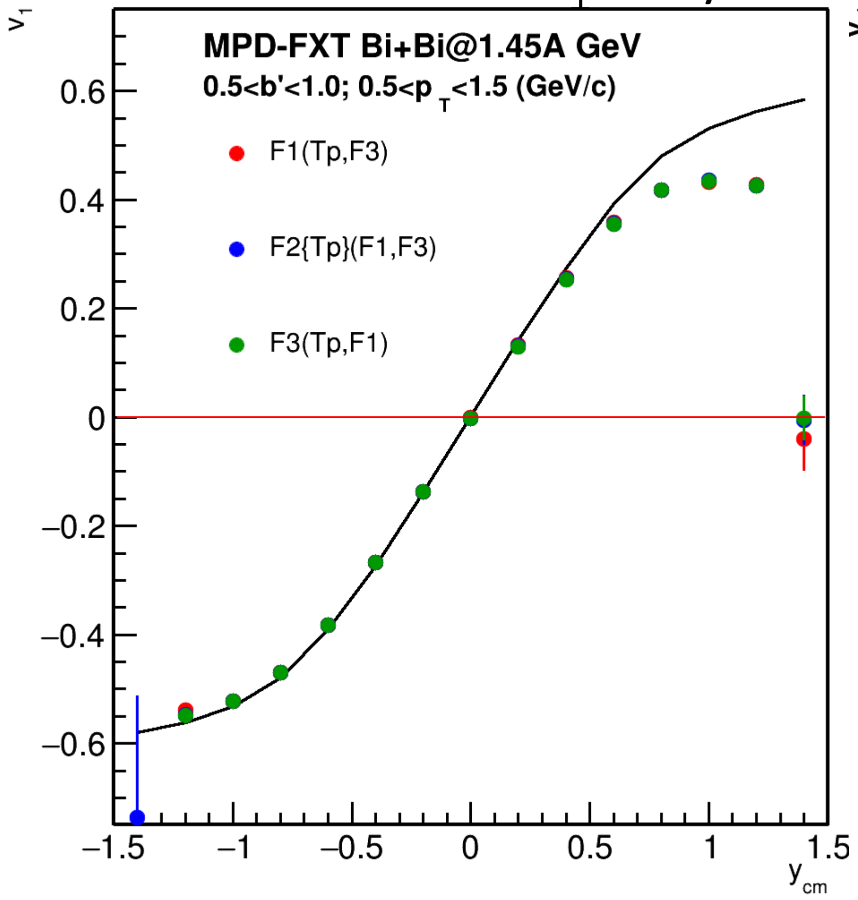

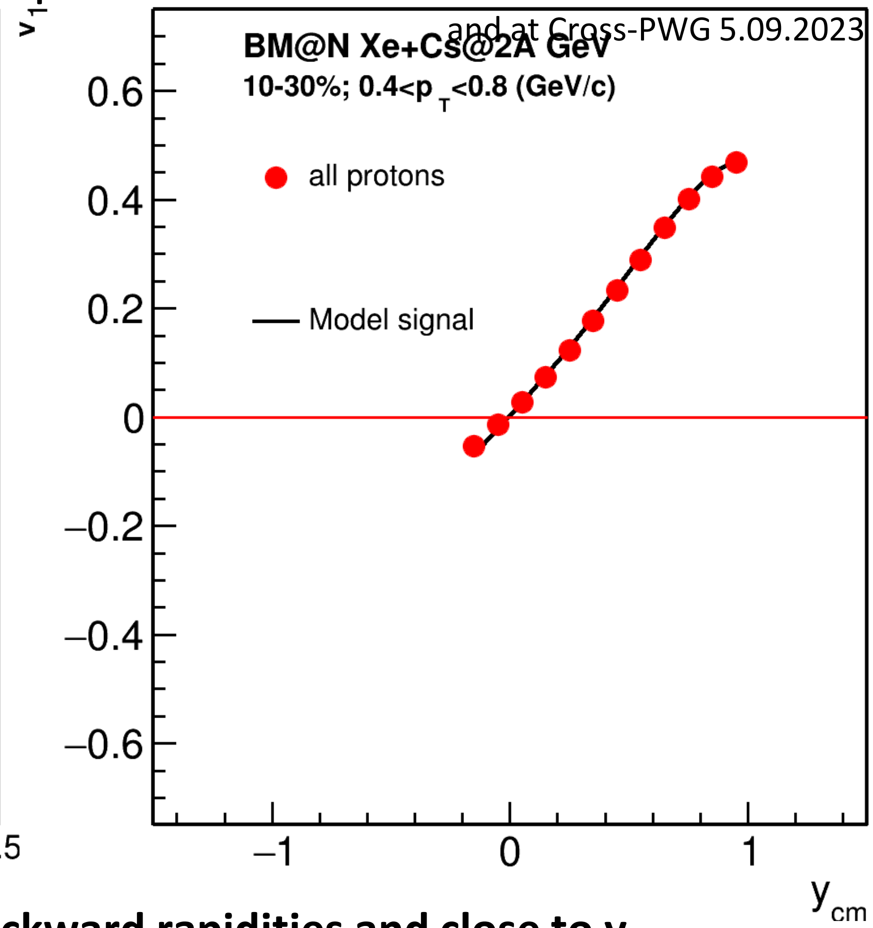

MPD has better coverage in backward rapidities and close to y_{beam}

MPD-FXT: v_2 for protons

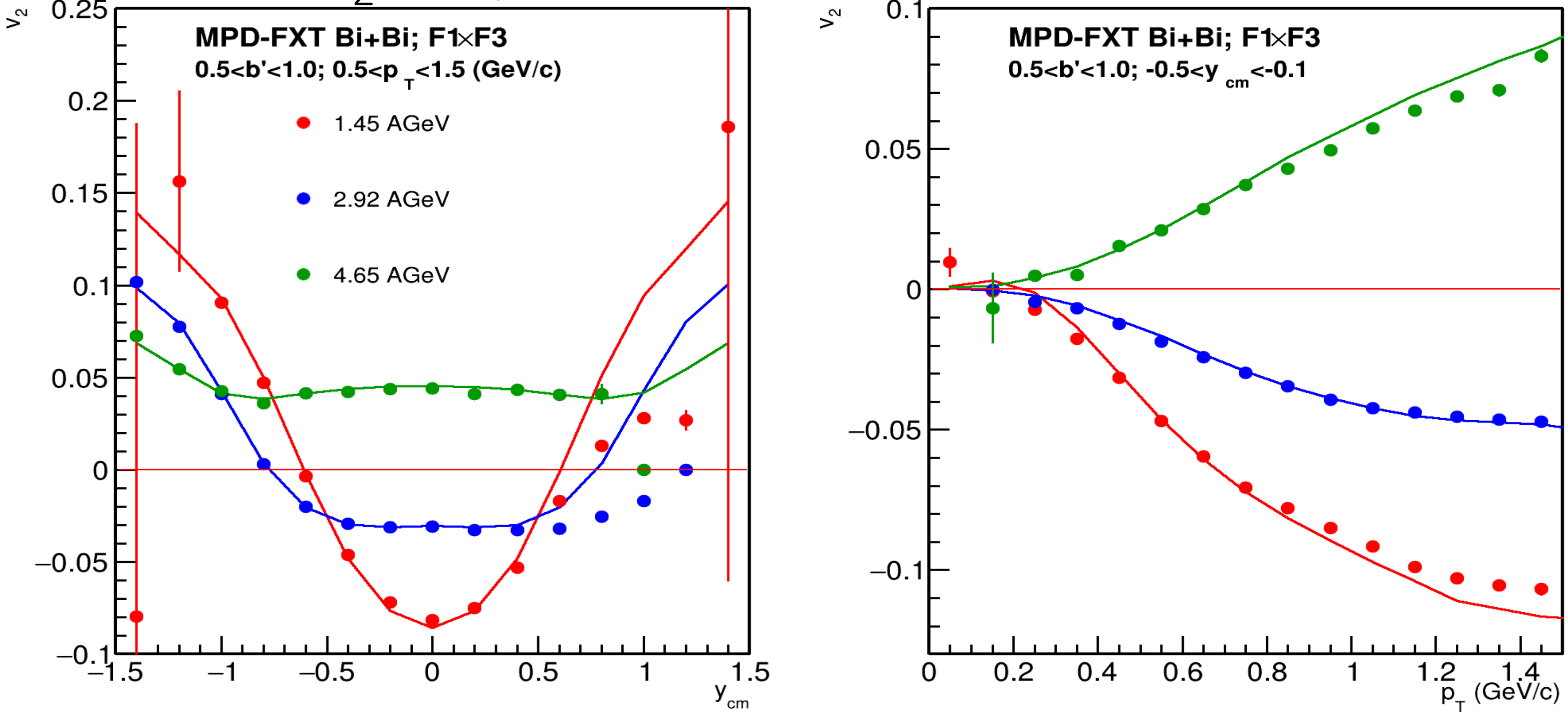

v_2 is consistent with model signal for y < 0.5

No efficiency corrections were applied yet

BM@N vs MPD: v_2 vs y for protons

See M.Mamaev's talk at ISHEP-2023
and at Cross-PWG 5.09.2023

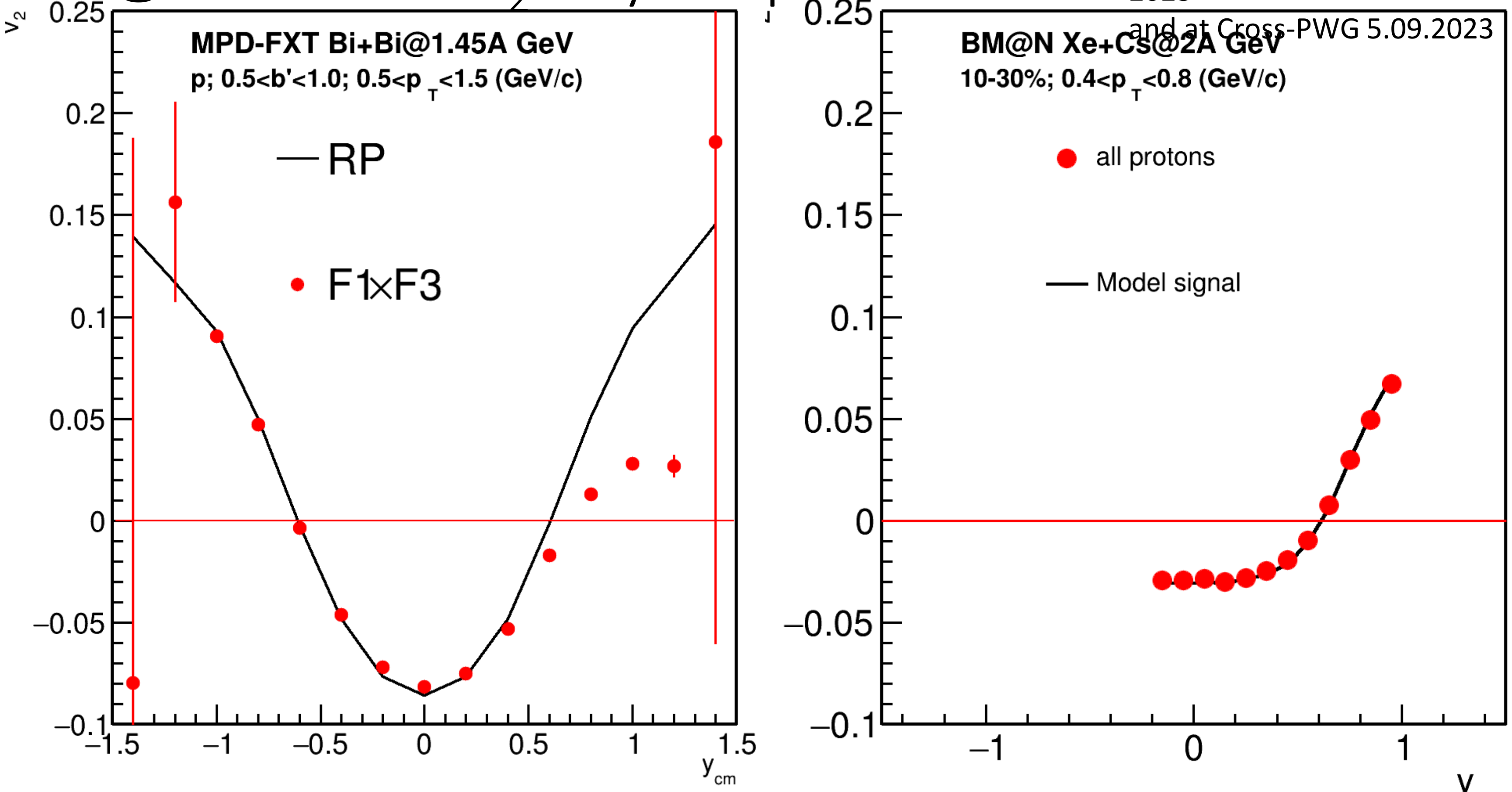

MPD has better coverage in backward rapidities and close to y_{beam}

Summary for the main topic 3

- **Performance study for v_n measurements using FFD detector:**
  - Event plane Resolution of FFD is much more smaller than FHCal resolution;
  - Good agreement for 2 and 3 sub event methods
  - FFD has extremely small Resolution for 2-nd harmonic
  - FFD can be used for directed flow measurements
  - FFD needs more statistics than FHCal for elliptic flow measurements due to low resolution
- **Performance study for v_n measurements in MPD-FXT:**
  - For each particle species v_1 and v_2 are consistent with the model signal mostly in backward rapidities
  - Official production for different beam energies ($\sqrt{s_{NN}}$=2.5, 3.0, 3.5 GeV 10-11 M min bias events each) has been requested for the further studies

Thank you for your attention!

Backup

Main topic 2: Elliptic flow fluctuations at NICA energies

Methods for v_n measurements

- **Sub-event 2-particle Q-cumulants v2{2}:** Δη=0.1 is applied between 2 sub-events A, B to suppress non-flow

$$Q_n = \sum_{i=1}^{M} e^{in\phi} \qquad \langle 2 \rangle_{a|b} = \frac{Q_{n_a} Q^*_{n,b}}{M_a M_b}$$

$$v_2\{2\} = \sqrt{\langle\langle 2 \rangle\rangle_{a|b}}$$

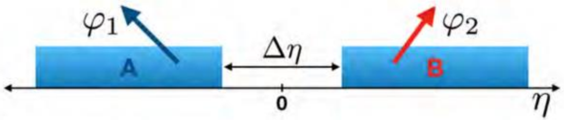

- **4-particle Q-cumulants v2{4}**

$$\langle 2 \rangle = \frac{|Q_n|^2 - M}{M(M-1)}$$

$$\langle 4 \rangle = \frac{|Q_n|^4 + |Q_{2n}|^2 - 2\Re[Q_{2n} Q_n^* Q_n^*] - 4(M-2)|Q_n|^2 - 2M(M-3)}{M(M-1)(M-2)(M-3)}$$

$$v_2\{4\} = \sqrt[4]{2\langle\langle 2 \rangle\rangle^2 - \langle\langle 4 \rangle\rangle}$$

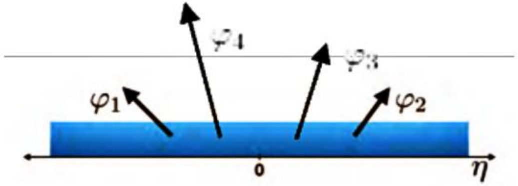

Method's details described in PRC 83 (2011), 044913 , EP method: Phys.Rev.C 77 (2008) 034904

Motivation of elliptic flow fluctuation study

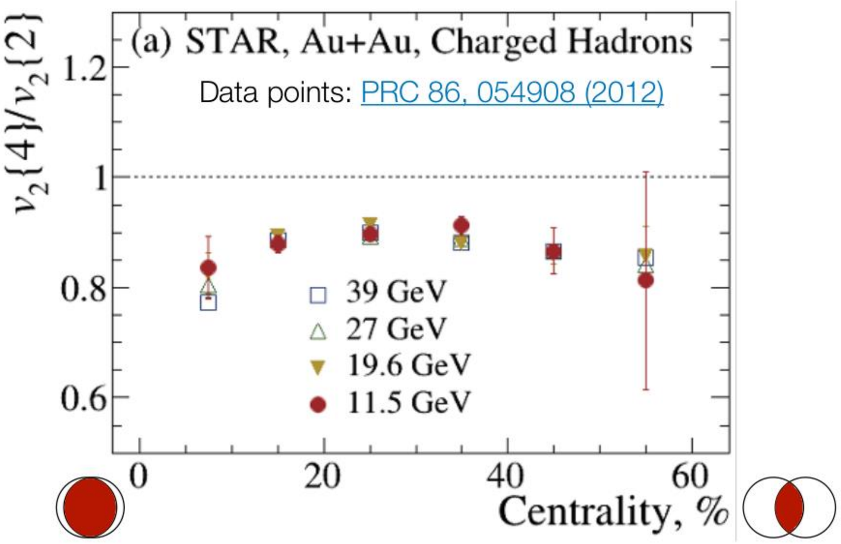

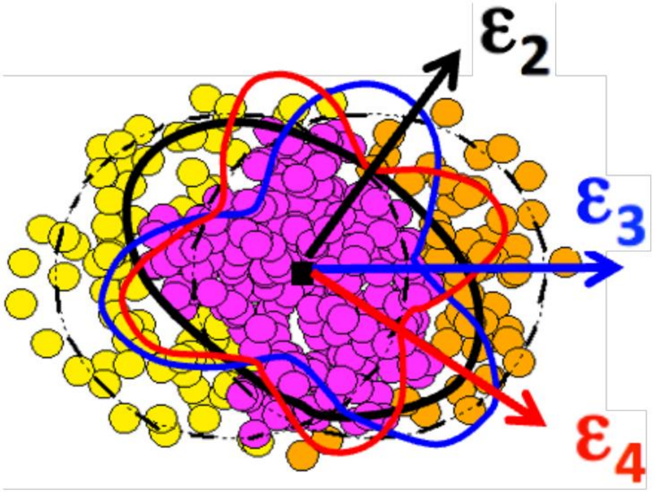

v_2 fluctuations at $\sqrt{s_{NN}} = 11.5 - 39$ GeV observed in STAR:

- Weak dependence on collision energy

- Indicate a dominated initial state driven uctuations $\sigma_{\varepsilon 2}$
- Provide constraints for IS models and shear viscosity η(T/s)

How about v2 fluctuations at NICA energies?

v_2 fluctuations at $\sqrt{s_{NN}}$ = 5 - 11.5 GeV

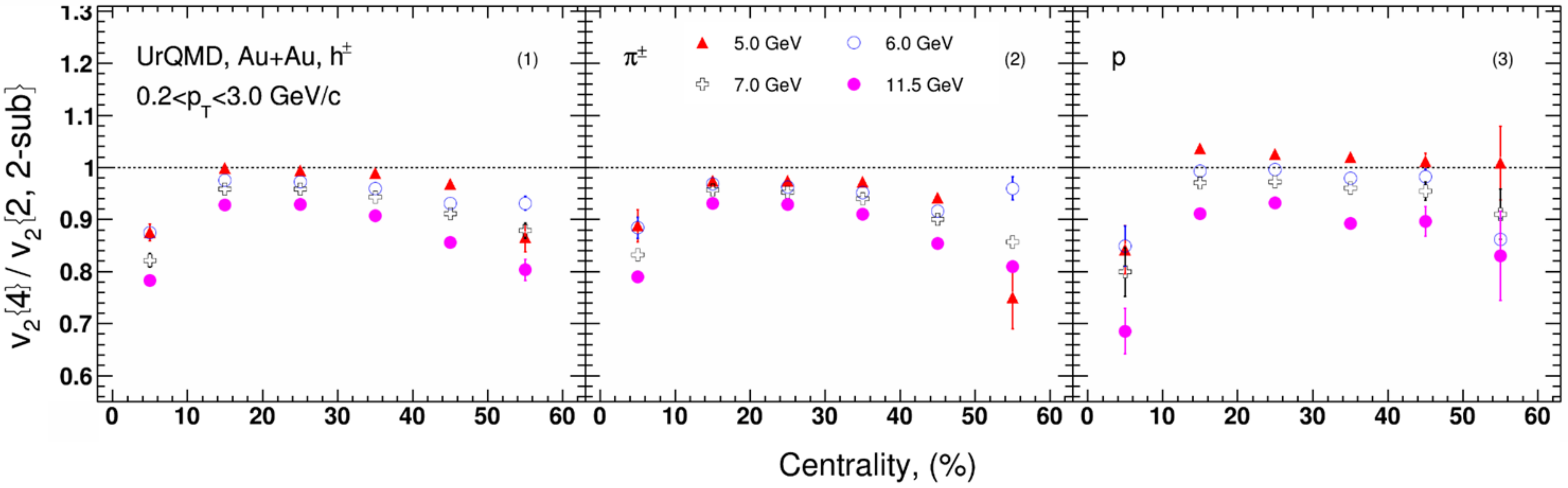

- v_2 fluctuations decrease with decreasing energy more strongly than at $\sqrt{s_{NN}}$ = 11.5-39 GeV
- The energy dependence of the $v_2\{4\}/v_2\{2\}$ is stronger for protons than for pions

Relative v_2 fluctuations of identified hadrons

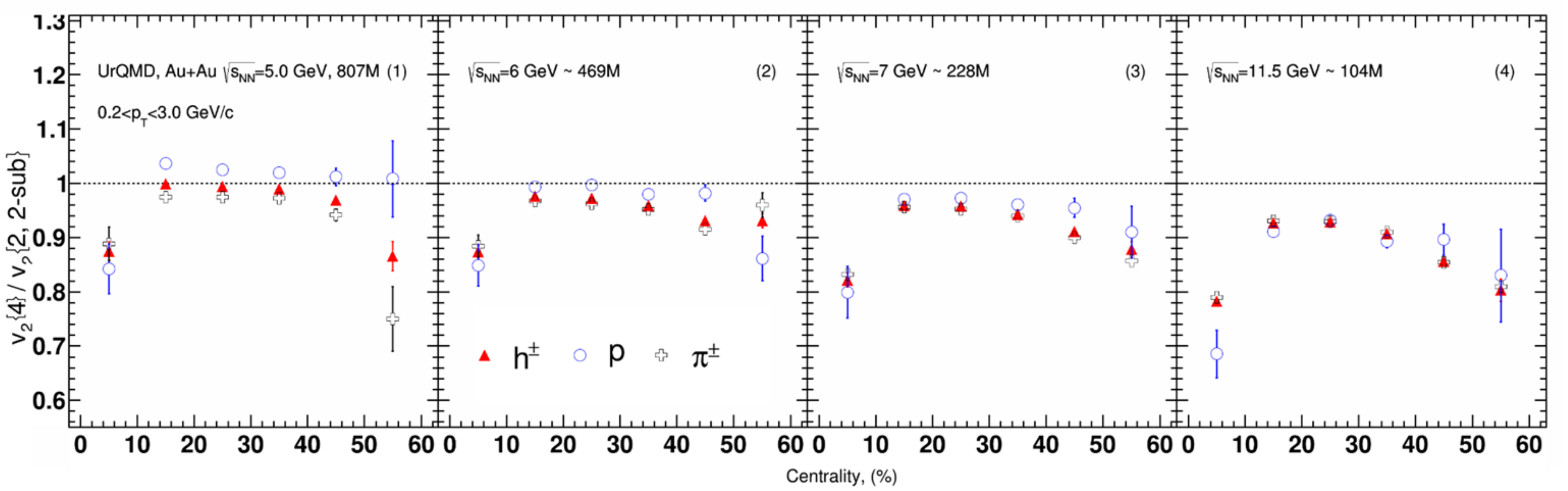

- Weak dependence between $v_2\{4\}/v_2\{2\}$ of protons and pions at 11.5 GeV
- The difference between $v_2\{4\}/v_2\{2\}$ of protons and pions increases with decreasing energy

Main topic 3: Study of the corrections for the non-uniform acceptance in the flow measurements and their application for the MPD experiment

Non-uniform acceptance corrections

TPC

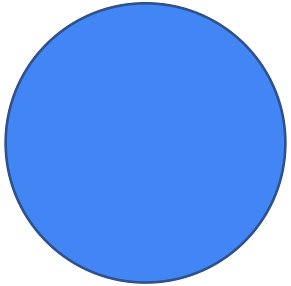

FHCal

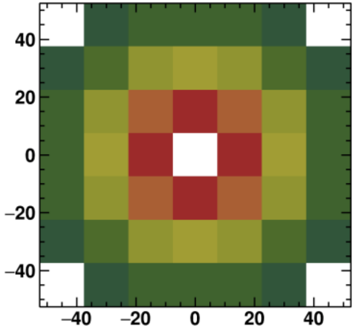

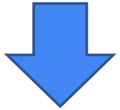

Acceptance filter

TPC

$-165° < \varphi < 165°$

FHCal

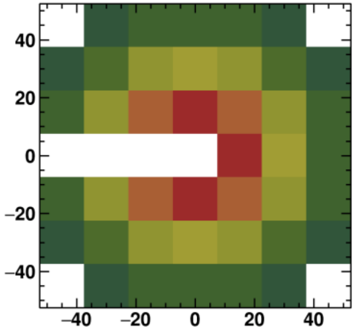

Modules 23, 24, 25 (L) and 19, 20, 21 (R) are off

Correction for non-uniform azimuthal acceptance

1. Recentering
1. Twist
1. Rescaling

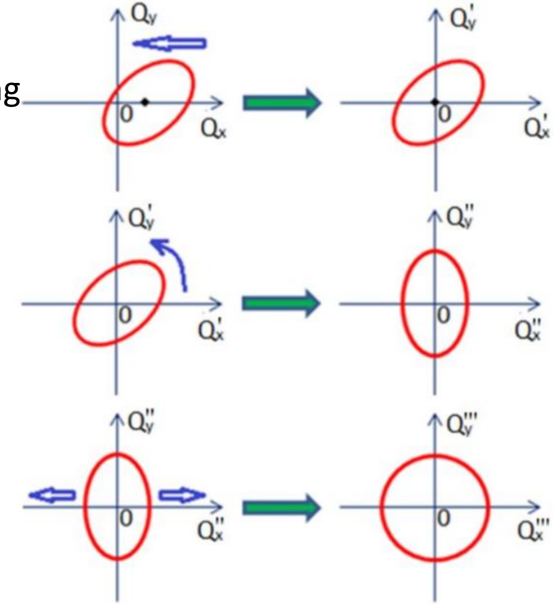

Corrections are based on method in:

I. Selyuzhenkov and S. Voloshin PRC77, 034904 (2008)

Effects of non-uniformity corrections; v_1 protons

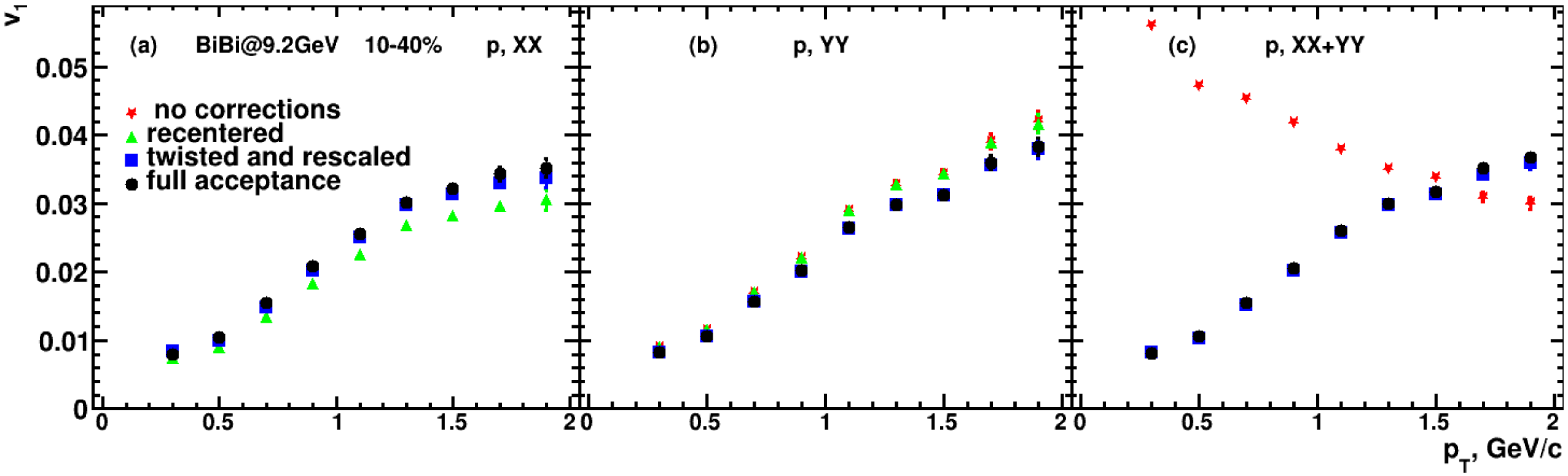

Effects of non-uniformity corrections; v_2 protons

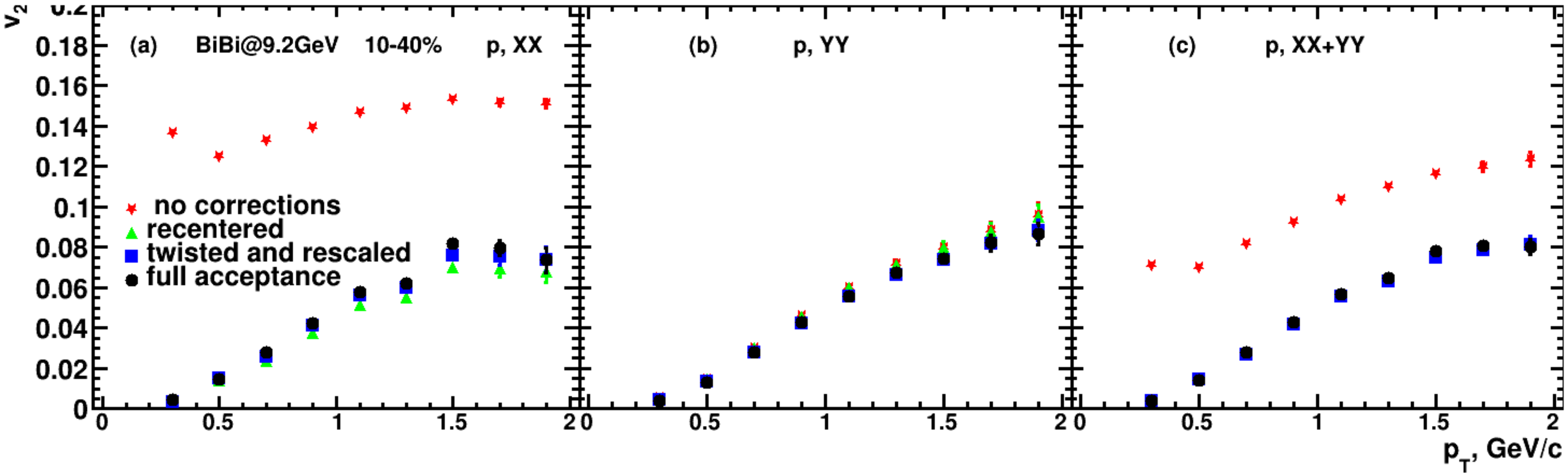

Correlation between global polarization and directed flow of **Λ**-hyperon

Global hyperon polarization

- w.r.t. reaction plane (RP)
- Emerges in HIC due to the system angular momentum
- Measured through the weak decay (1)

$$\frac{\mathrm{d}N}{\mathrm{d}\cos\theta^*} = \frac{1}{2}(1+\alpha_\mathrm{H}|\vec{P}_\mathrm{H}|\cos\theta^*) \quad (1)$$

$$\Lambda \to p + \pi^-$$

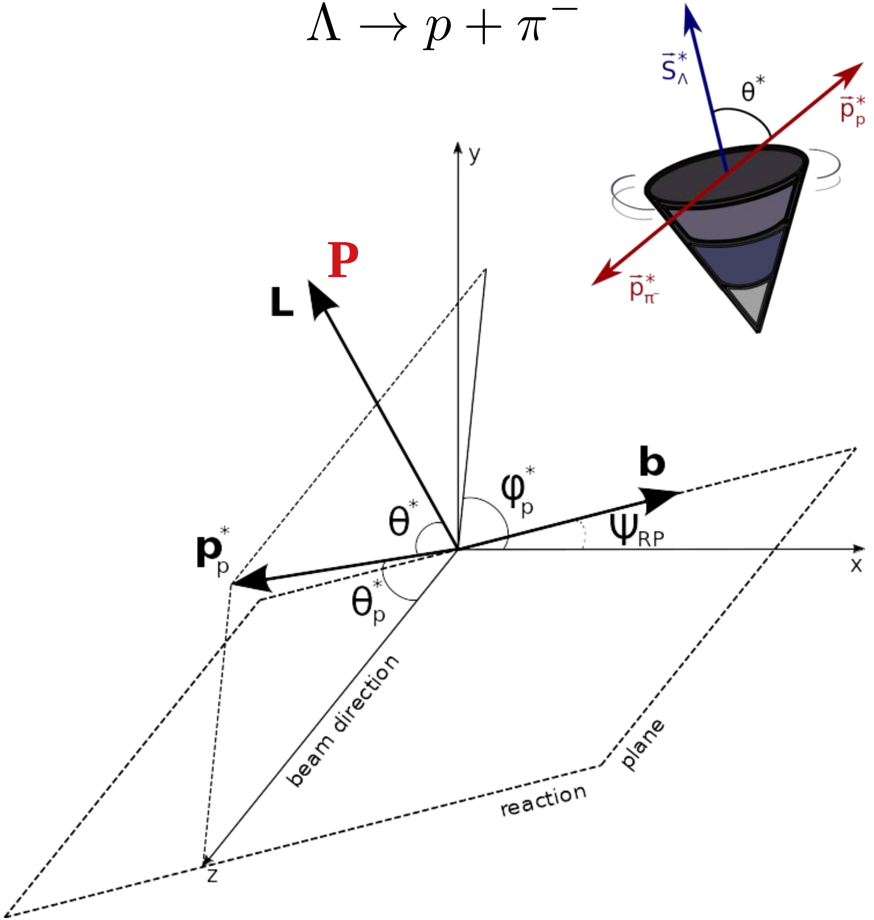

- * — denotes Lambda rest frame
- θ^* — angle between the decay particle and polarization direction
- $\alpha_\Lambda \simeq -\alpha_{\bar{\Lambda}} \simeq 0.732$ (Value updated in 2019)

Global Polarization at Nuclotron-NICA energies

- Predicted and observed global polarization signals rise as the collision energy is reduced:

  NICA energy range will provide new insight

- $\Lambda(\bar{\Lambda})$ - splitting of global polarization
- Comparison of models, detailed study of energy and kinematical dependences, improving precision
- Probing the vortical structure using various observables

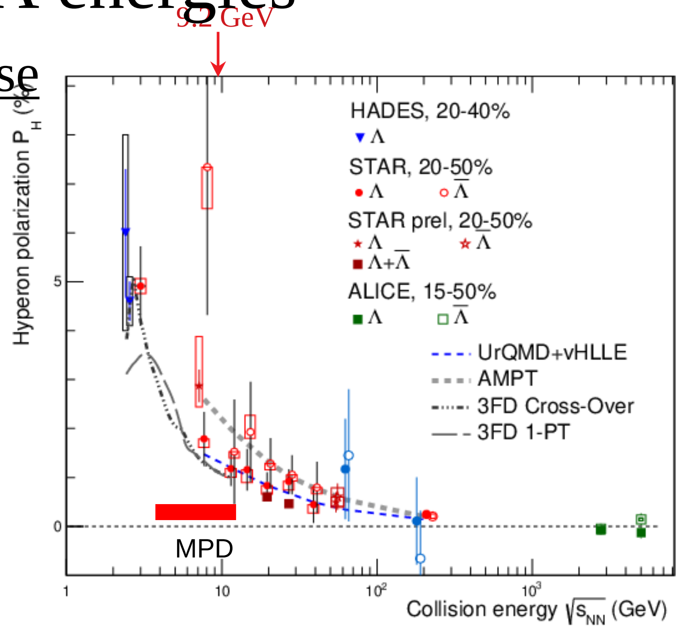

S. Singha, EPJ Web Conf. 276 (2023) 06012

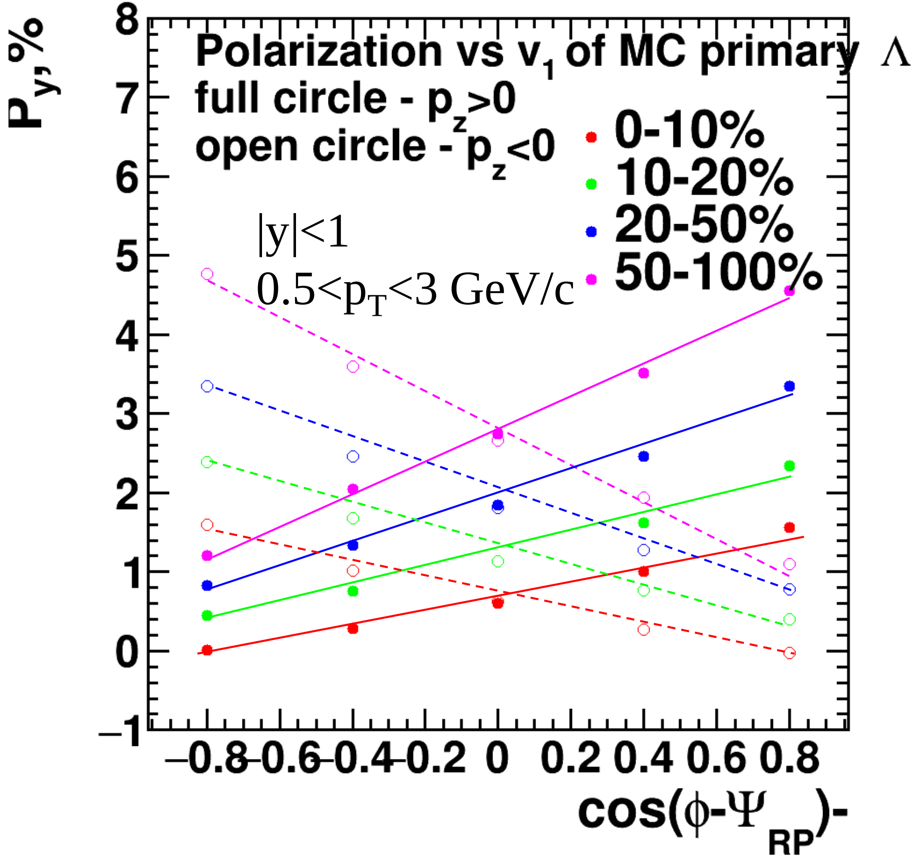

Pearson correlation coefficient represent linear correlation between two sets of data from -1 to 1

$$\rho(X,Y) = \frac{Cov(X,Y)}{Var(X)Var(Y)}$$

$$Cov(X,Y) = \langle XY \rangle - \langle X \rangle \langle Y \rangle$$

$$Var(X) = \sqrt{\langle X^2 \rangle - \langle X \rangle^2}$$

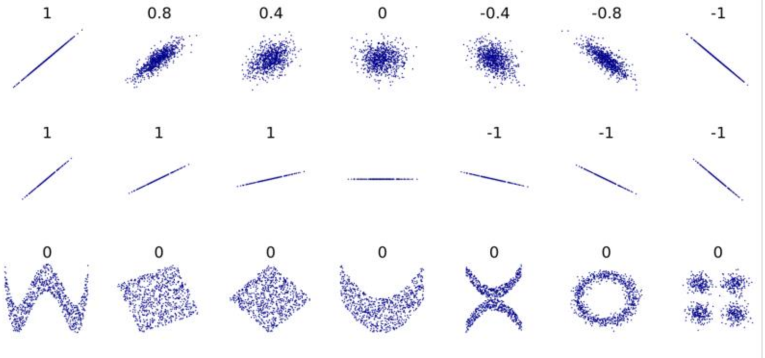

P_y vs p_T and P_y vs y in centrality classes

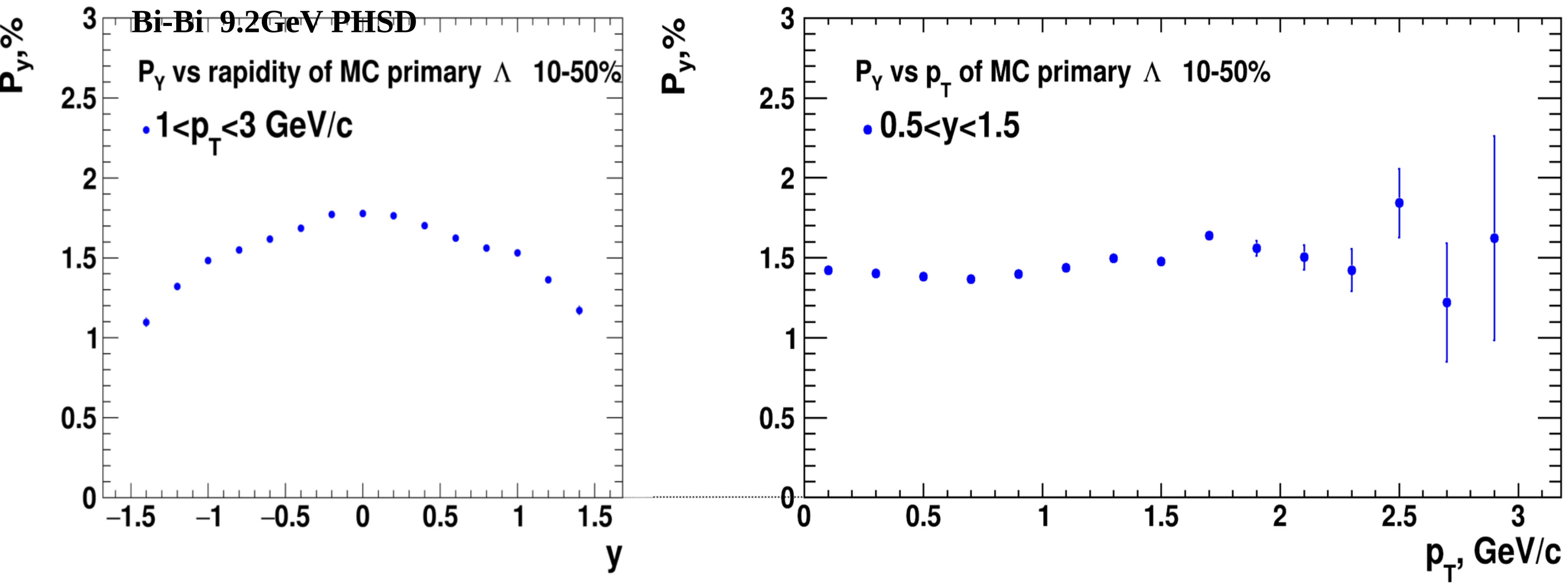

- Weak dependence on p_T
- Highest signal in mid-rapidity

v_1 vs p_T and v_1 vs y in centrality classes

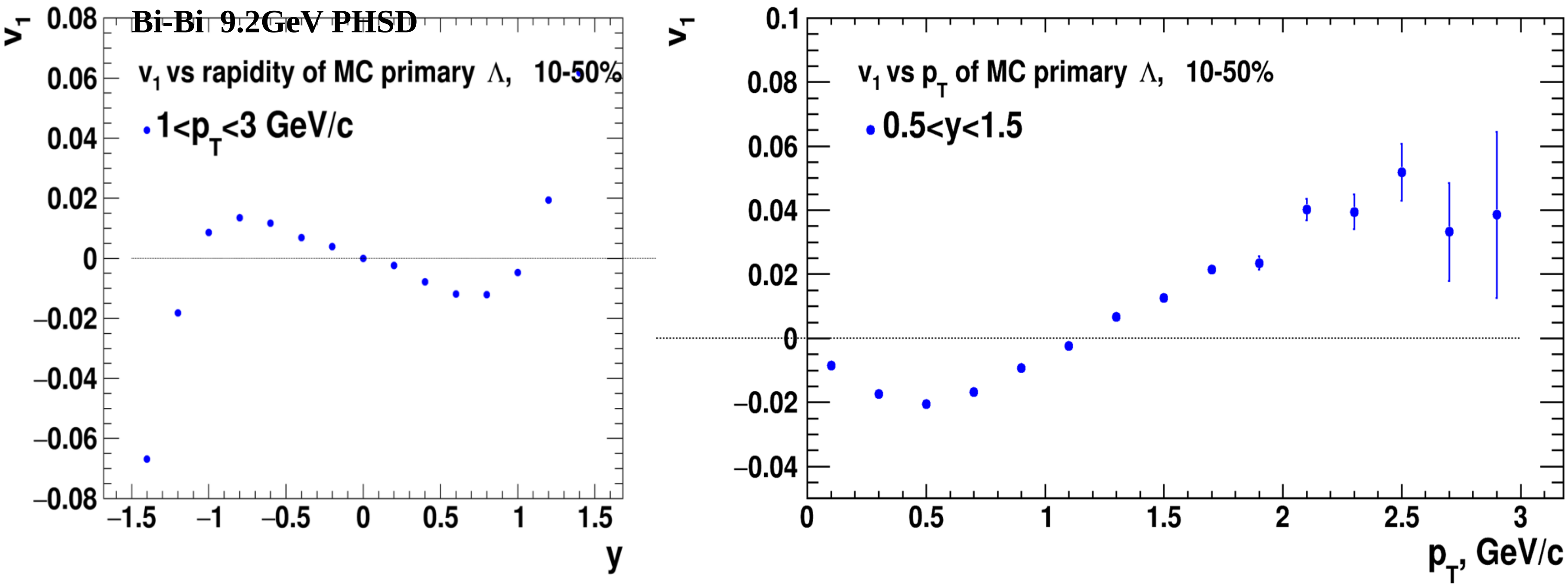

- Small signal of directed flow
- Better to investigate p_T>1.2 GeV/c

Pearson correlation coefficient between P, v_1 and N

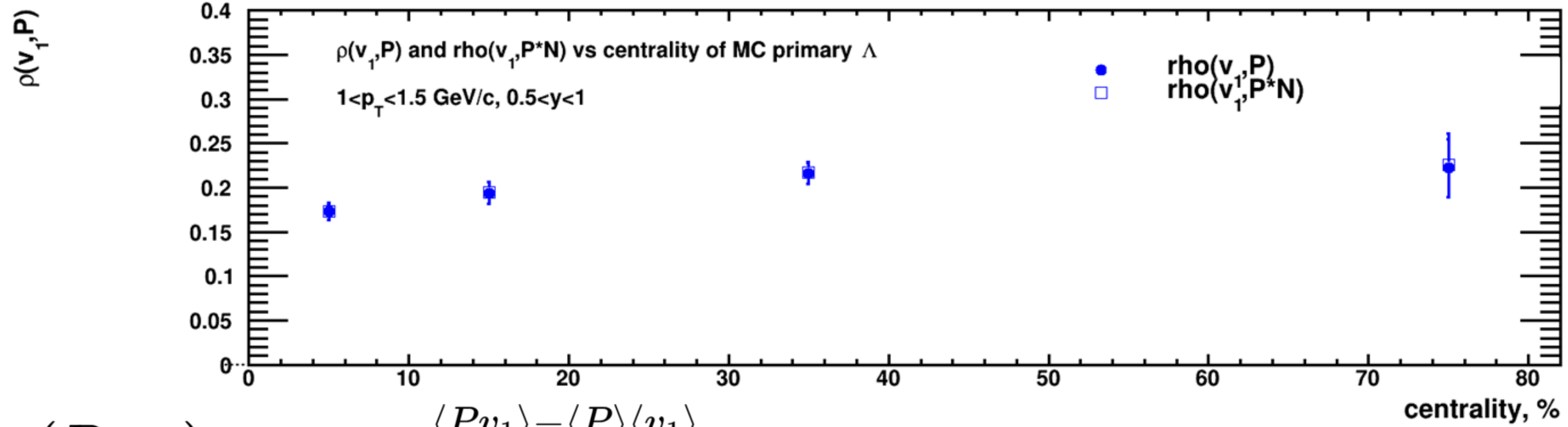

$$\rho(P, v_1) = \frac{\langle Pv_1\rangle - \langle P\rangle\langle v_1\rangle}{(\sqrt{\langle v_1^2\rangle - \langle v_1\rangle^2})(\sqrt{\langle P^2\rangle - \langle P\rangle^2})}$$

N - multiplicity of Primary Λ

$$\rho(P, v_1 * N) = \frac{\rho(P,v_1) - \rho(P,N)\rho(v_1,N)}{(\sqrt{1-\rho(P,N)^2})(\sqrt{1-\rho(v_1,N)^2})}$$

- Weak centrality dependence of Pearson correlation coefficient

Pearson correlation coefficient between P_y and v_1

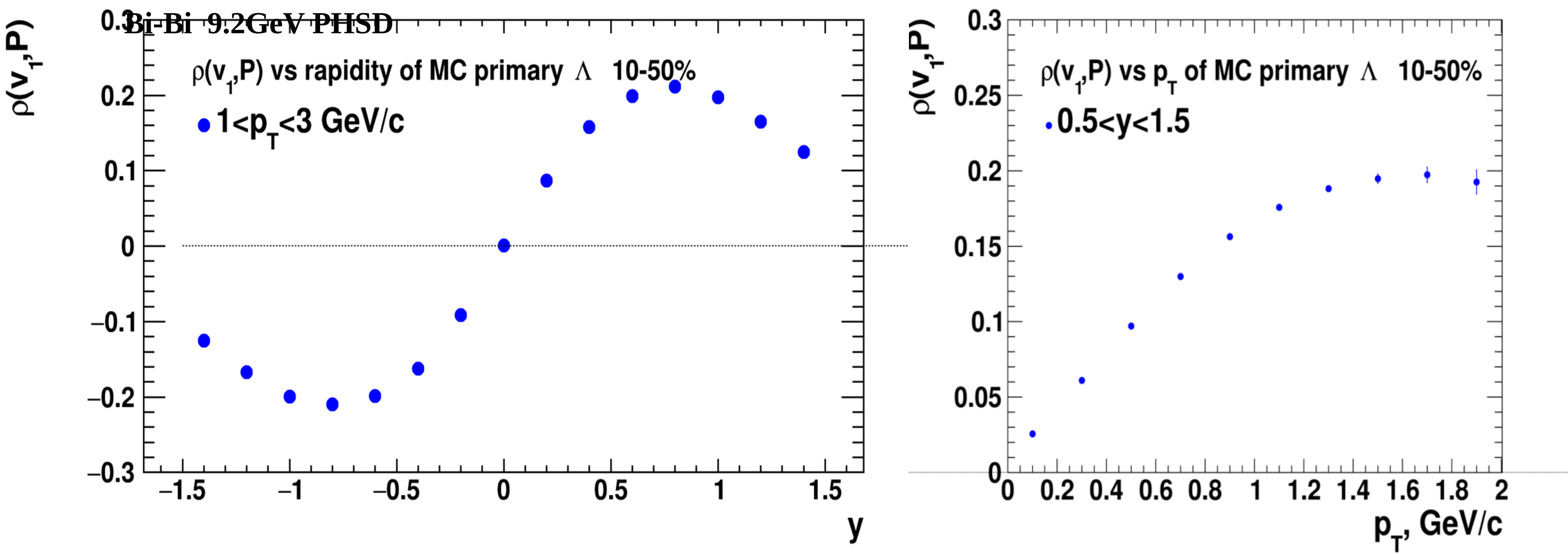

$$\rho(P, v_1) = \frac{\langle P v_1 \rangle - \langle P \rangle \langle v_1 \rangle}{(\sqrt{\langle v_1^2 \rangle - \langle v_1 \rangle^2})(\sqrt{\langle P^2 \rangle - \langle P \rangle^2})}$$

- moderate linear dependence between P_y and v_1
- increasing with p_T
- highest for $0.5<y<1$

Summary

- Small v_1 in mid-rapidity and for $0<p_T<1$ GeV/c
- Weak p_T dependence for P_y, highest signal in mid-rapidity
- Moderate linear dependence between P_y and v_1
- Effect of multiplicity of Primary Λ is negligible

Outlook

- Further investigation of different effects in correlation between P_y and v_1
- Search another correlation parameter

Simplified MC sampling for hadron calorimeters

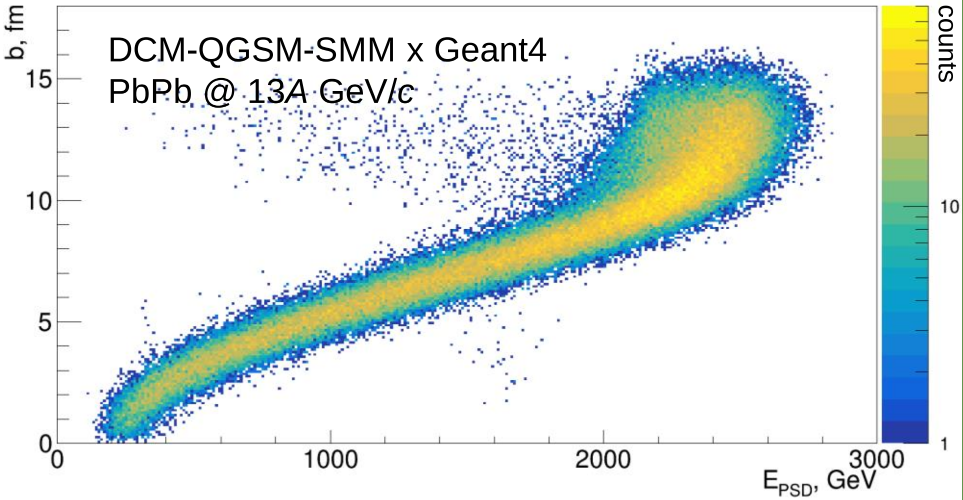

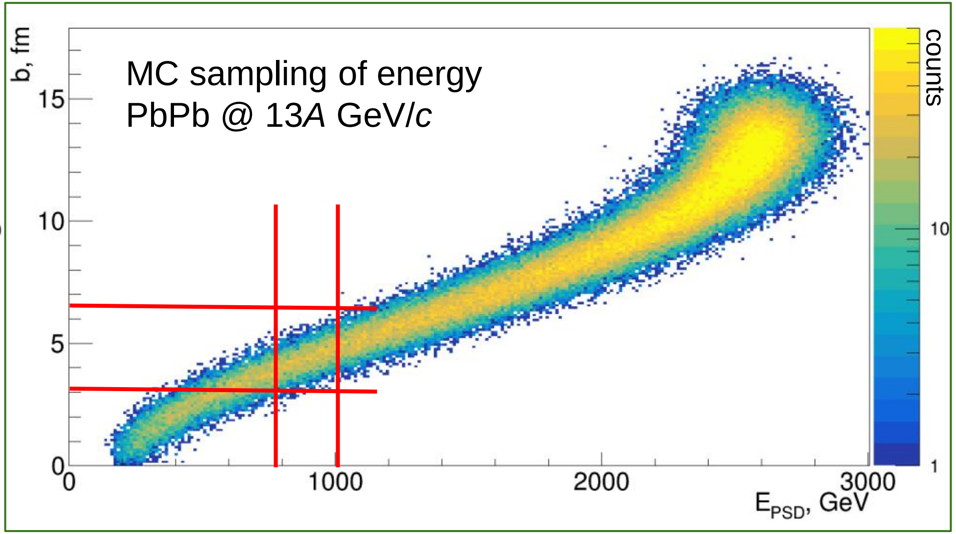

- Shapes of energy and impact parameter distributions are similar
- Width of distribution for energy is larger than for multiplicity
- Possible decrease of width will be study

NA61/SHINE experimental setup

Data samples:

- Pb-Pb @ p_{beam} = 13A GeV/c
- data from 2016 physics run
- DCM-QGSM-SMM x Geant4
  M.Baznat et al. PPNL 17 (2020) 3, 303

Subsystems

- Multiplicity: TPCs
- Spectators energy: PSD

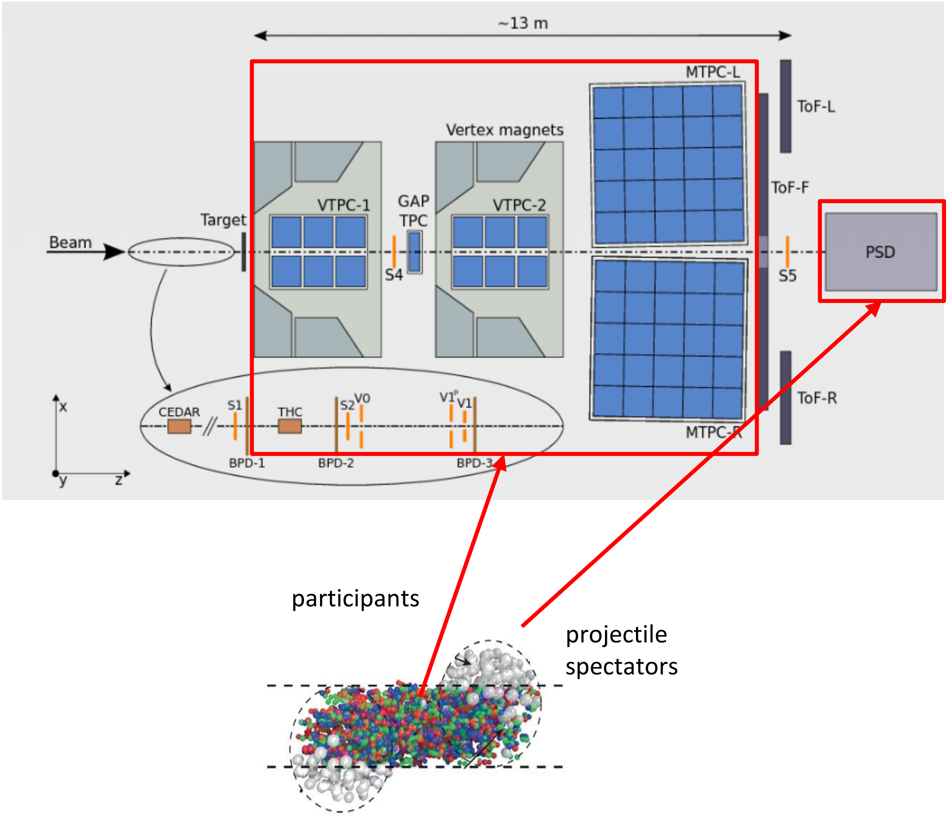

General distributions: Event

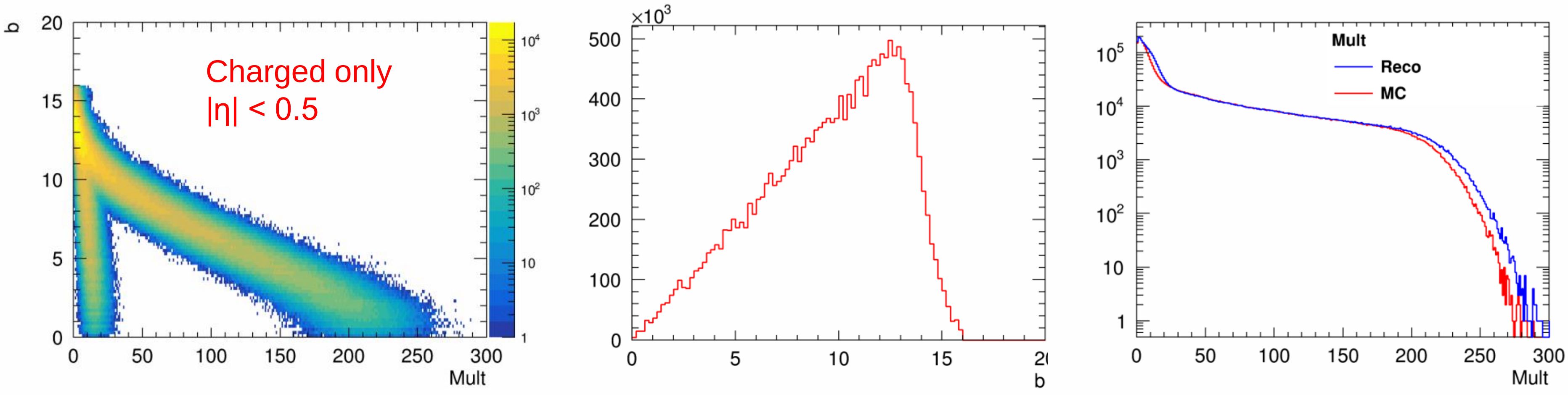

Observed a non-physical tail in the distribution Mult vs b

General distributions: Tracks

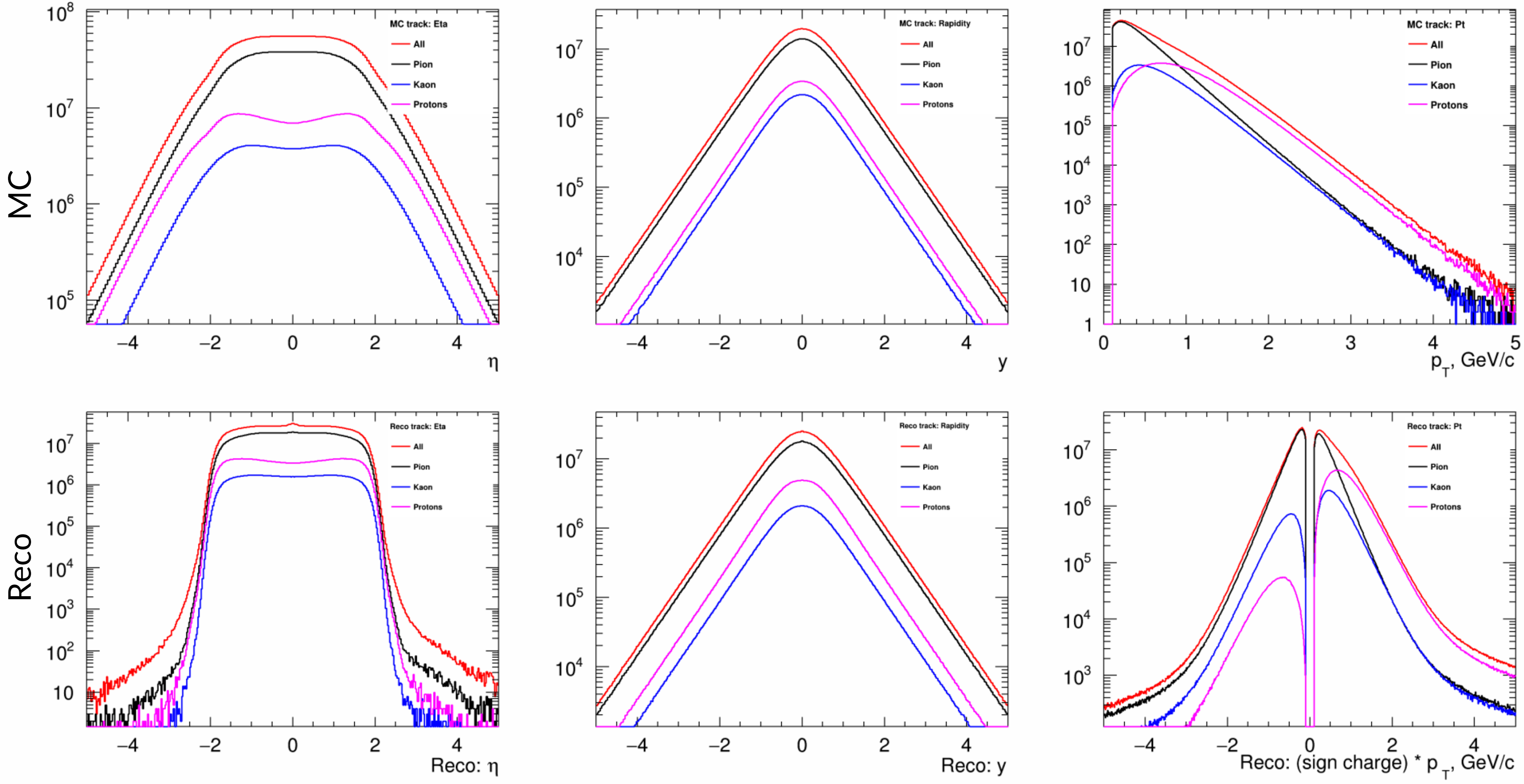

Centrality determination

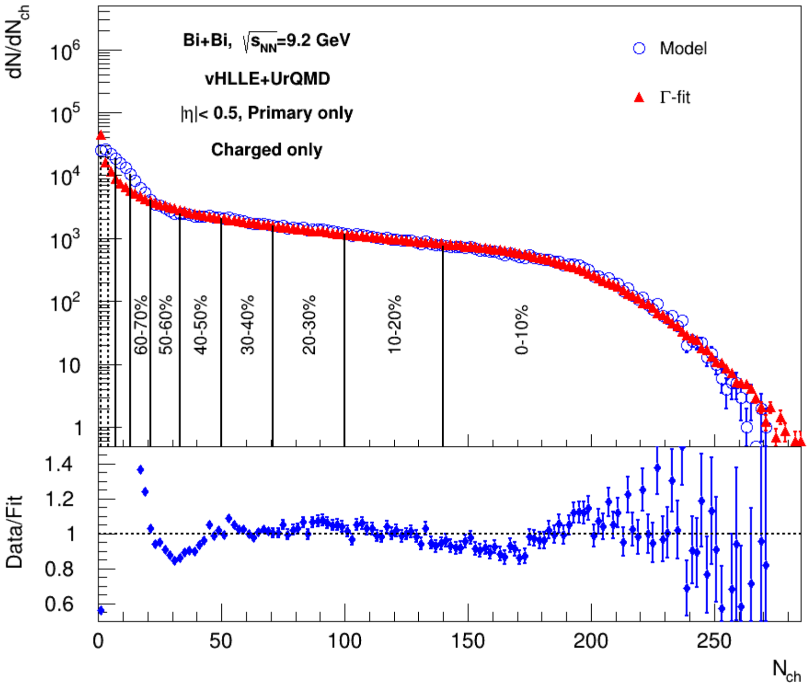

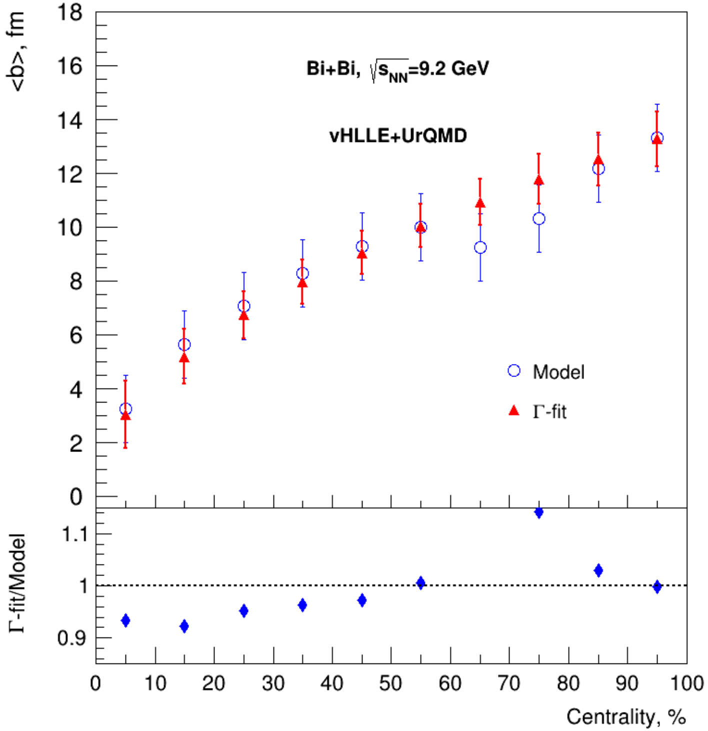

The reasonable fit quality and good agreement of the impact parameter distribution with the model data for 0-60% centrality classes.

Comparison of Reco and MC: $v_2\{2,|\Delta\ \eta|>0.2\}$

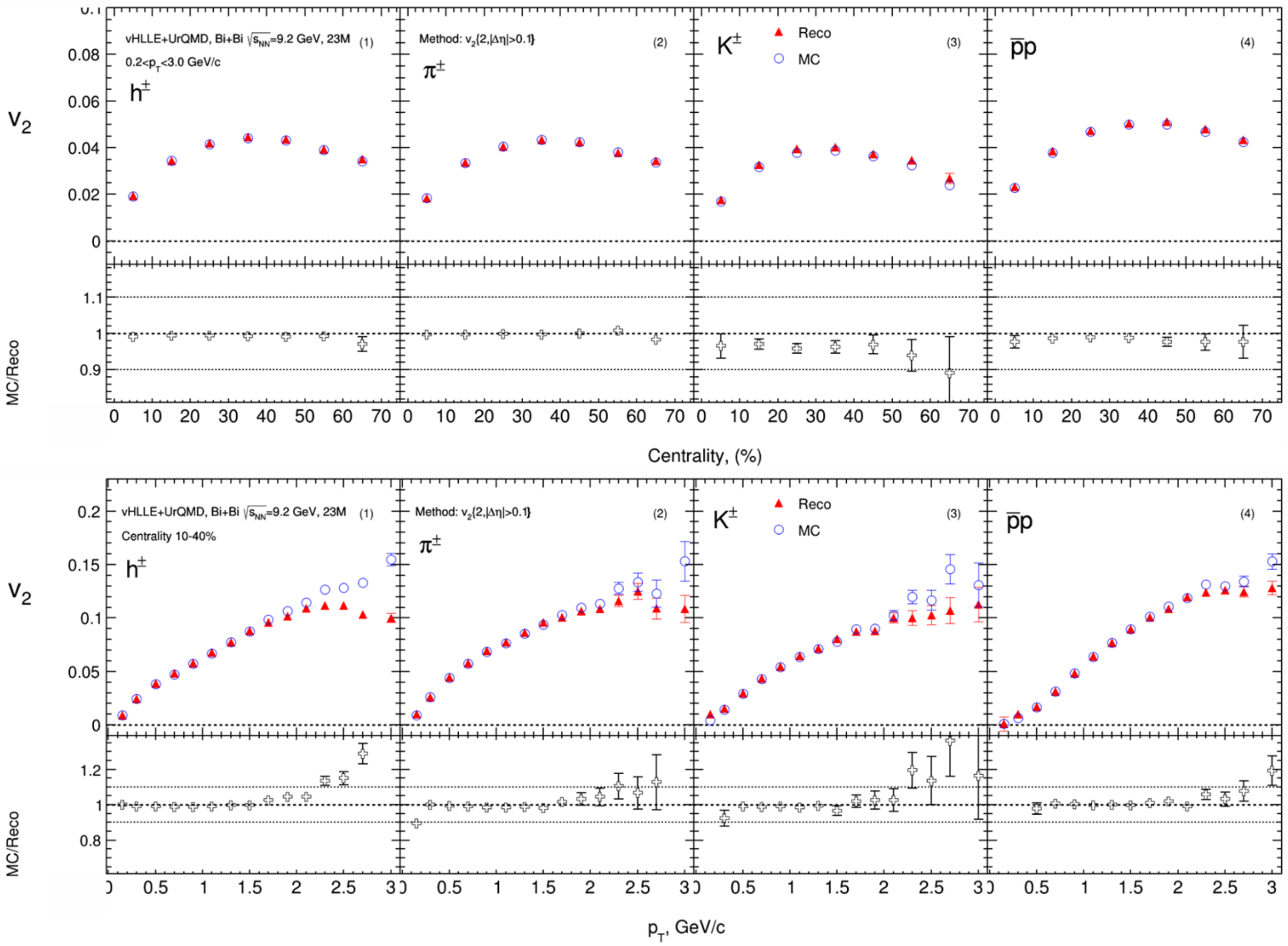

Cuts:

- Charged particles only
- Primary
- $|\Delta\ \eta|$ = 0,1
- $\Delta\ \eta$ = 0,1
- p_T >0.2 GeV/c
- $|DCA|<3\sigma$
- nTPC hits ≥ 16
- PID: PDG code

❑ good agreement of the $v_{2,mc}$ with $v_{2,reco}$ data

❑ The difference at large p_T betwin $v_{2,mc}$ and $v_{2,reco}$ (non-flow ?)

Comparison of Reco and MC: $v_2\{4\}$

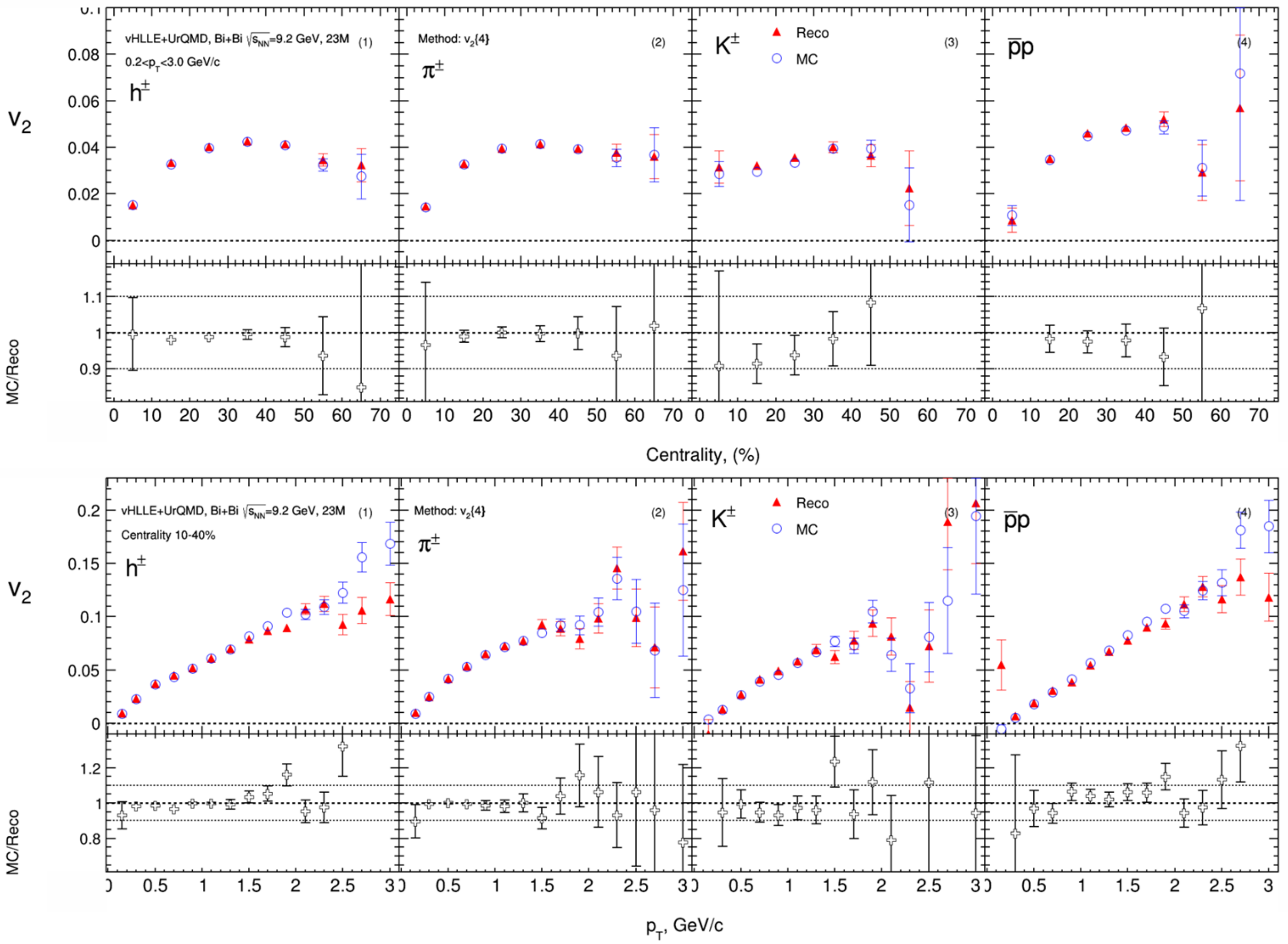

Cuts:

- Charged particles only
- Primary
- $|\eta|<1.5$
- $\Delta\,\eta = 0{,}1$
- $p_T > 0.2$ GeV/c
- $|DCA|<3\sigma$
- nTPC hits ≥ 16
- PID: PDG code

❑ good agreement of the $v_{2,mc}$ with $v_{2,reco}$ data

❑ The difference at large p_T betwin $v_{2,mc}$ and $v_{2,reco}$ is less than for other methods -> Not affected by the non-flow effects

u_n, Q_n vectors formalism for flow measurements

- Unit vector of a particle $u_n(\text{centrality}, \text{pid}, p_T, y)$:

$$u_n = e^{in\varphi} = \begin{cases} u_{n,x} \equiv x_n = \cos n\varphi \\ u_{n,y} \equiv y_n = \sin n\varphi \end{cases}$$

- Event flow vector $Q_n(\text{centrality})$:

$$Q_n = \sum_{k=1}^{M} \omega_n^k u_n^k \equiv |Q_n| e^{in\Psi_n} = \begin{cases} Q_{n,x} \equiv X_n = |Q_n| \cos n\Psi_n \\ Q_{n,y} \equiv Y_n = |Q_n| \sin n\Psi_n \end{cases}$$

- φ – azimuthal angle of the produced particle
- ω – weight of the Q_n vector (for example, $\omega = 1$ for participant plane and $\omega = E$ for spectator plane)
- Ψ_n – event plane angle

More information:
https://inspirehep.net/literature/757158

FHCal & FFD event plane Resolution for v_1

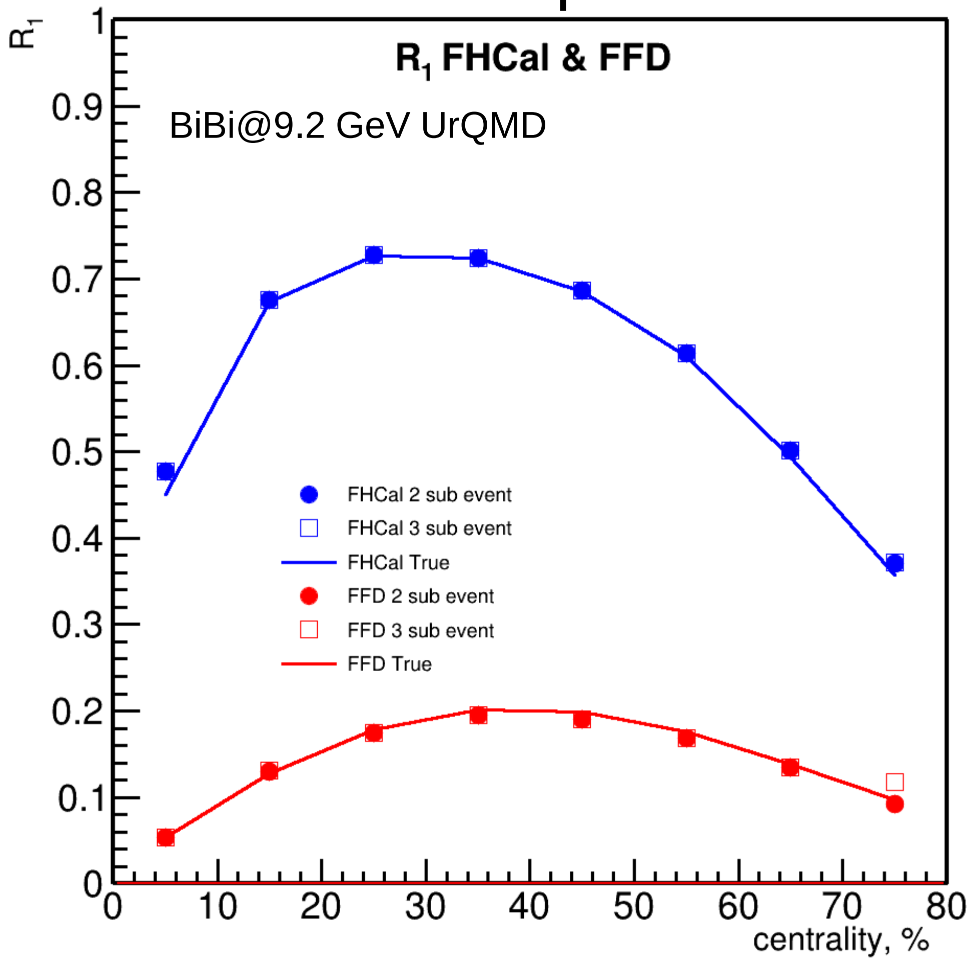

2 sub event

$$R_{1,i} = \sqrt{\langle Q^N_{1,i} Q^S_{1,i} \rangle}, i = x, y$$

$$R^{True}_{1,i} = \langle Q_{1,i} \Psi_{RP} \rangle$$

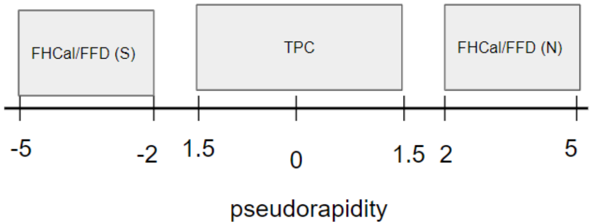

3 sub event

$$R^N_{1,i} = \sqrt{\frac{2\langle Q^N_{1,i} Q^S_{1,i} \rangle \langle Q^S_{1,i} Q^{TPC}_{1,i} \rangle}{\langle Q^N_{1,i} Q^{TPC}_{1,i} \rangle}}$$

- FFD resolution are smaller than FHCal
- 2 and 3 sub event has good agreement with True Resolution

FHCal & FFD event plane Resolution for v_2

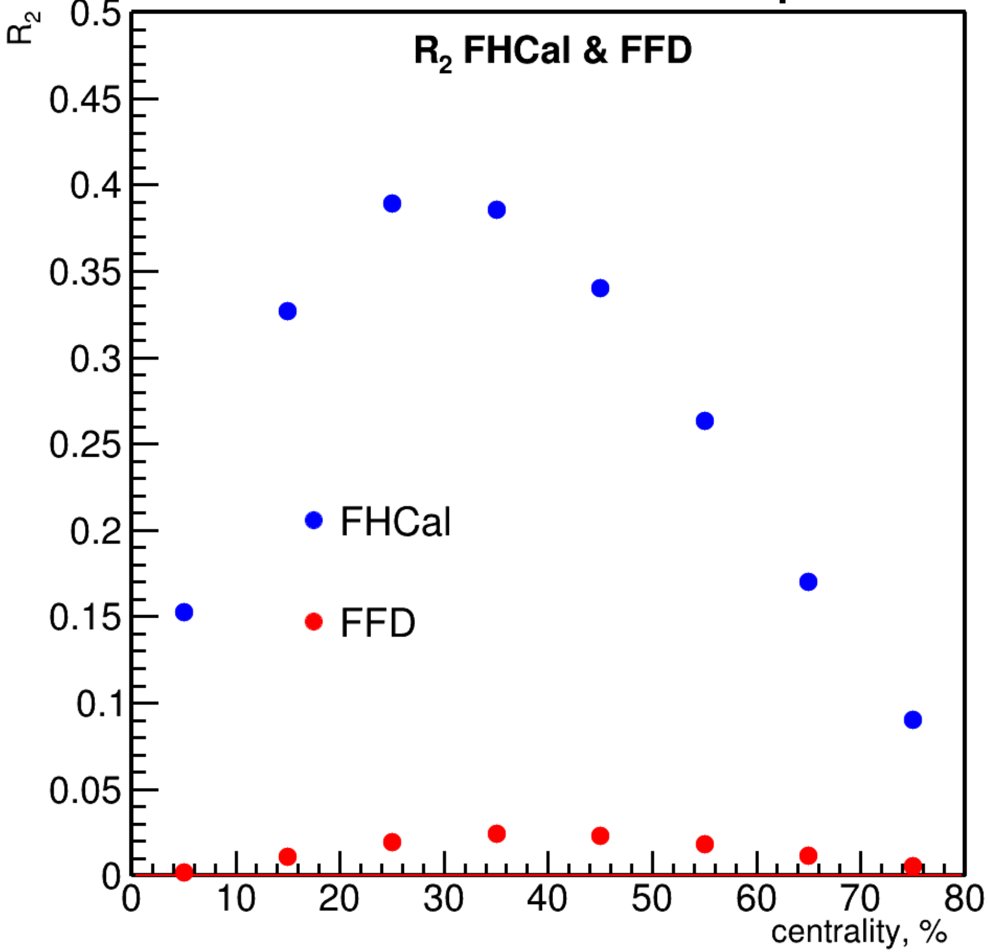

Extrapolation to obtain R_2

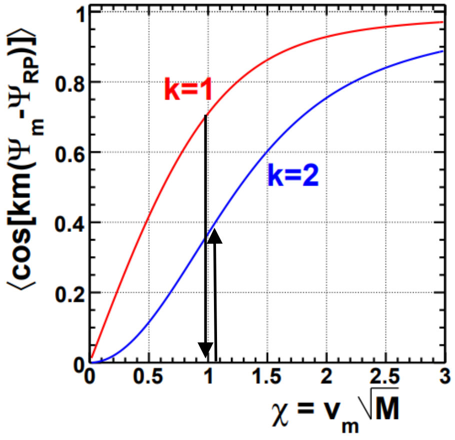

- FFD resolution is extremely small.

The BM@N experiment (GEANT4 simulation for RUN8)

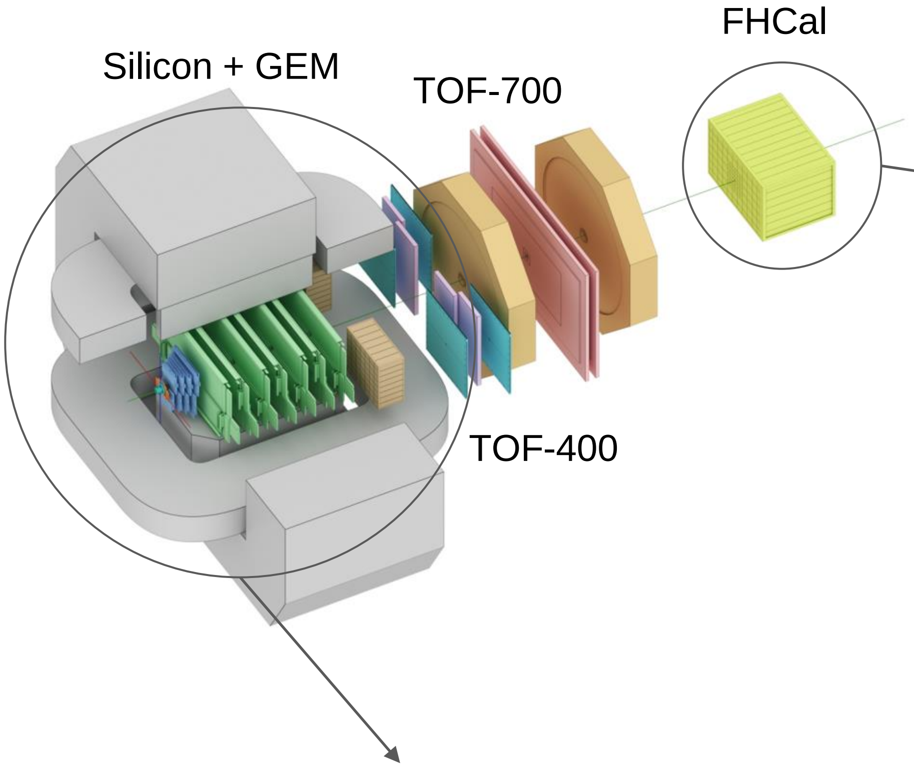

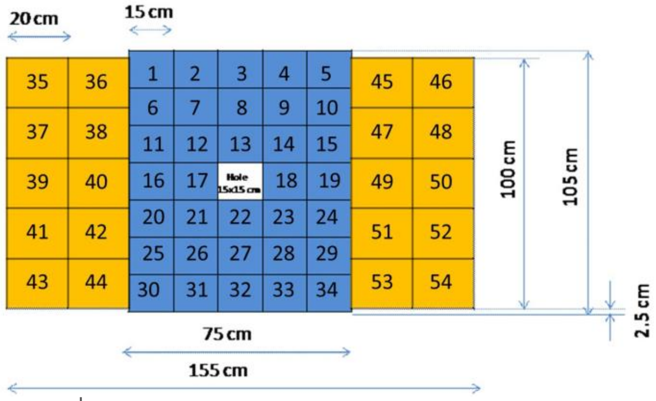

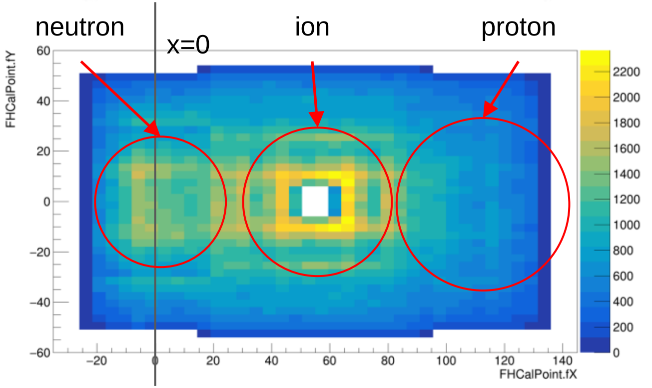

Square-like tracking system within the magnetic field deflecting particles along X-axis

Charge splitting on the surface of the FHCal is observed due to magnetic field

BM@N vs MPD: p_T-y acceptance

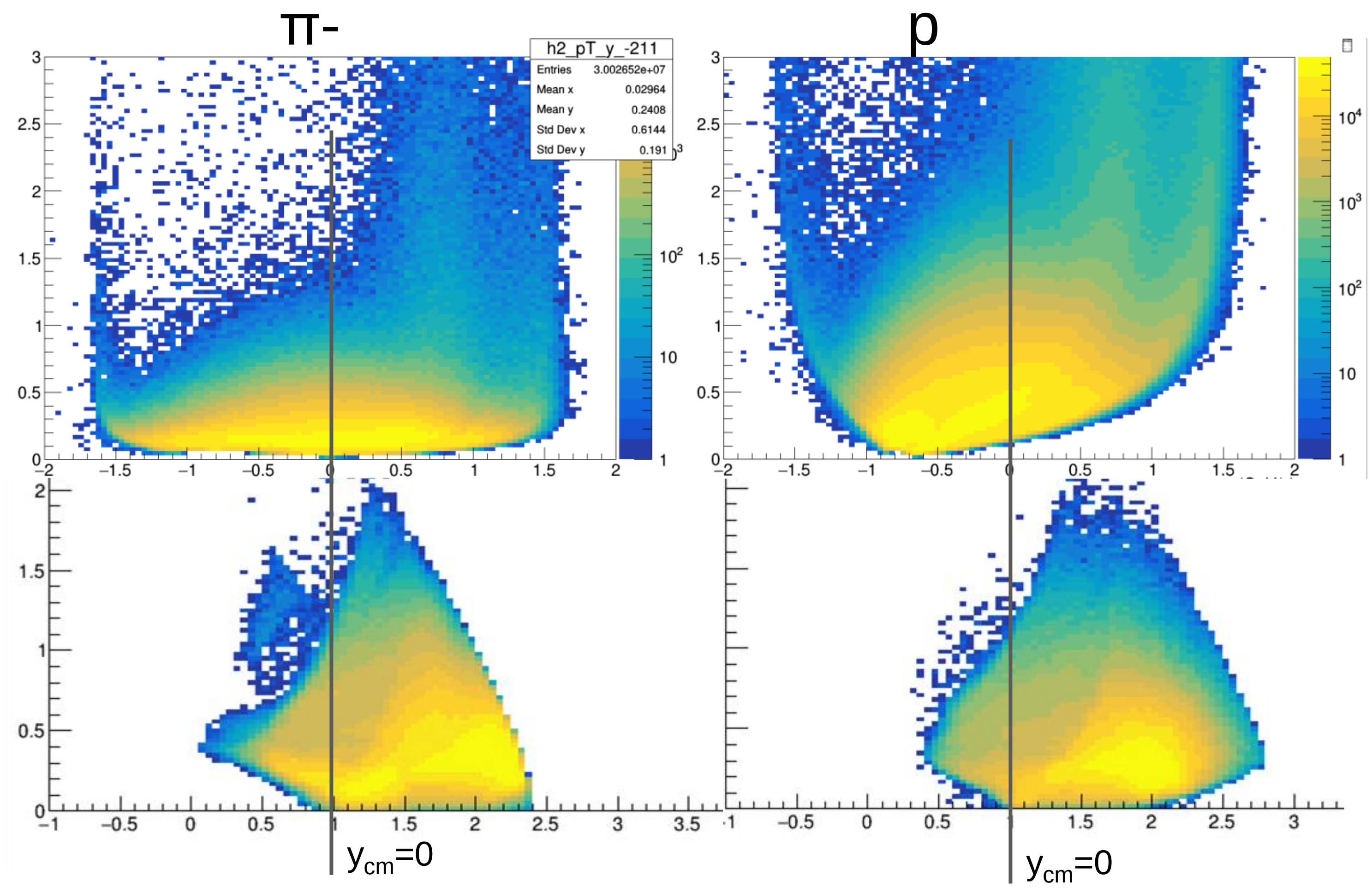

MPD has greater coverage of backward area (even covers projectile spectators) and MPD covers midrapidity region

BM@N has greater coverage of forward area

BM@N vs MPD: η-φ acceptance

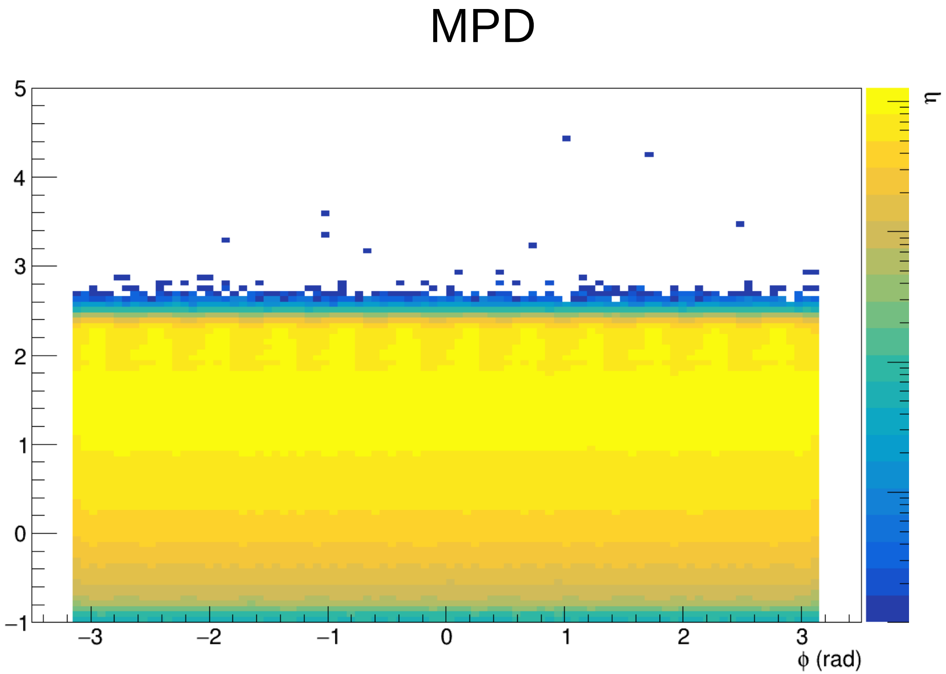

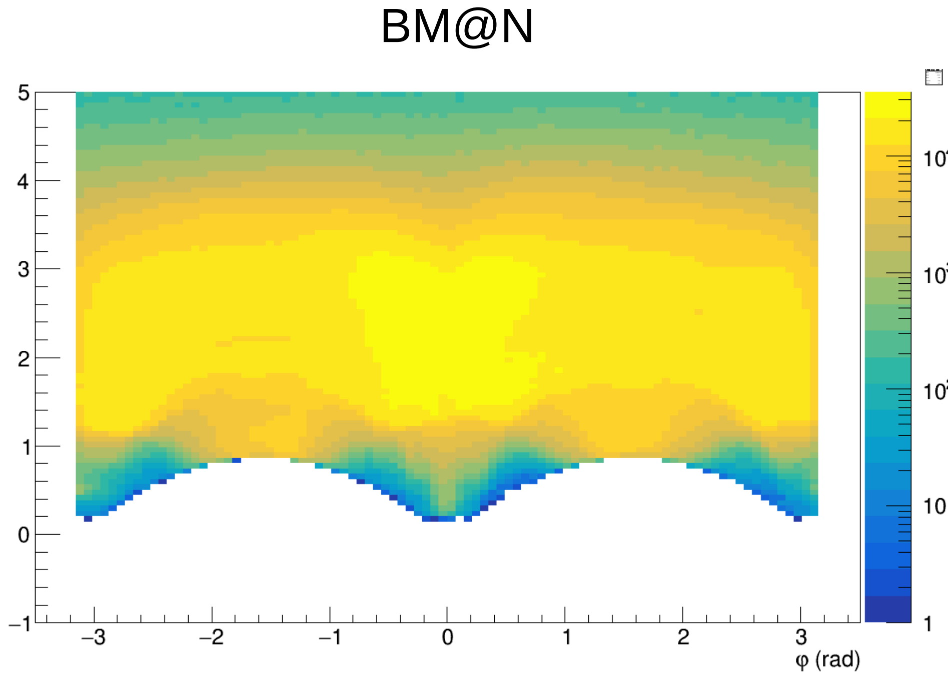

- MPD has more uniform acceptance along φ-axis
- BM@N has non-uniform acceptance due to square-like shape of the tracking system

Flow methods for v_n calculation

Tested in HADES:
M Mamaev et al 2020 PPNuclei 53, 277–281
M Mamaev et al 2020 J. Phys.: Conf. Ser. 1690 012122

Scalar product (SP) method:

$$v_1 = \frac{\langle u_1 Q_1^{F1} \rangle}{R_1^{F1}} \qquad v_2 = \frac{\langle u_2 Q_1^{F1} Q_1^{F3} \rangle}{R_1^{F1} R_1^{F3}}$$

Where R_1 is the resolution correction factor

$$R_1^{F1} = \langle \cos(\Psi_1^{F1} - \Psi_1^{RP}) \rangle$$

Symbol "F2(F1,F3)" means R_1 calculated via (3S resolution):

$$R_1^{F2(F1,F3)} = \frac{\sqrt{\langle Q_1^{F2} Q_1^{F1} \rangle \langle Q_1^{F2} Q_1^{F3} \rangle}}{\sqrt{\langle Q_1^{F1} Q_1^{F3} \rangle}}$$

Method helps to eliminate non-flow
Using 2-subevents doesn't

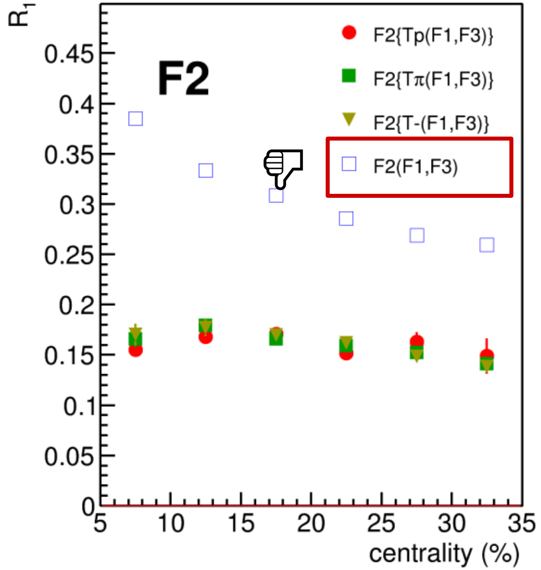

Symbol "F2{Tp}(F1,F3)" means R_1 calculated via (4S resolution):

$$R_1^{F2\{Tp\}(F1,F3)} = \langle Q_1^{F2} Q_1^{Tp} \rangle \frac{\sqrt{\langle Q_1^{F1} Q_1^{F3} \rangle}}{\sqrt{\langle Q_1^{Tp} Q_1^{F1} \rangle \langle Q_1^{Tp} Q_1^{F3} \rangle}}$$

SP: R_1 for FHCal spectator plane

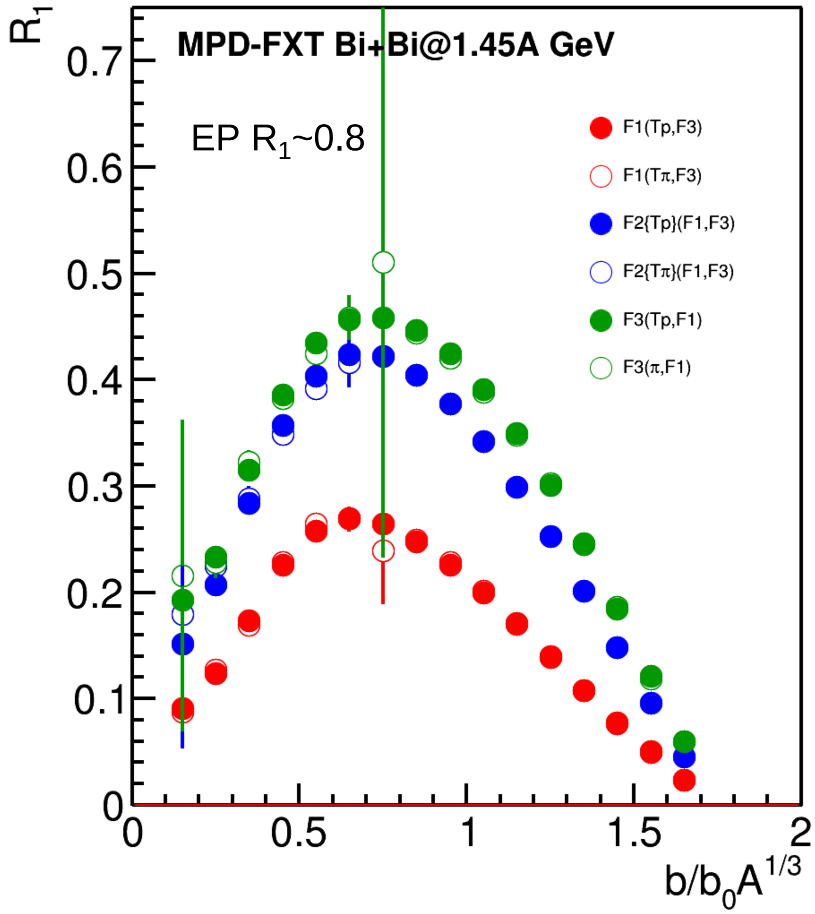

Good agreement between R_1 calculated using different combinations of Q-vectors with significant rapidity separation

BM@N vs MPD: v_1 vs y for protons

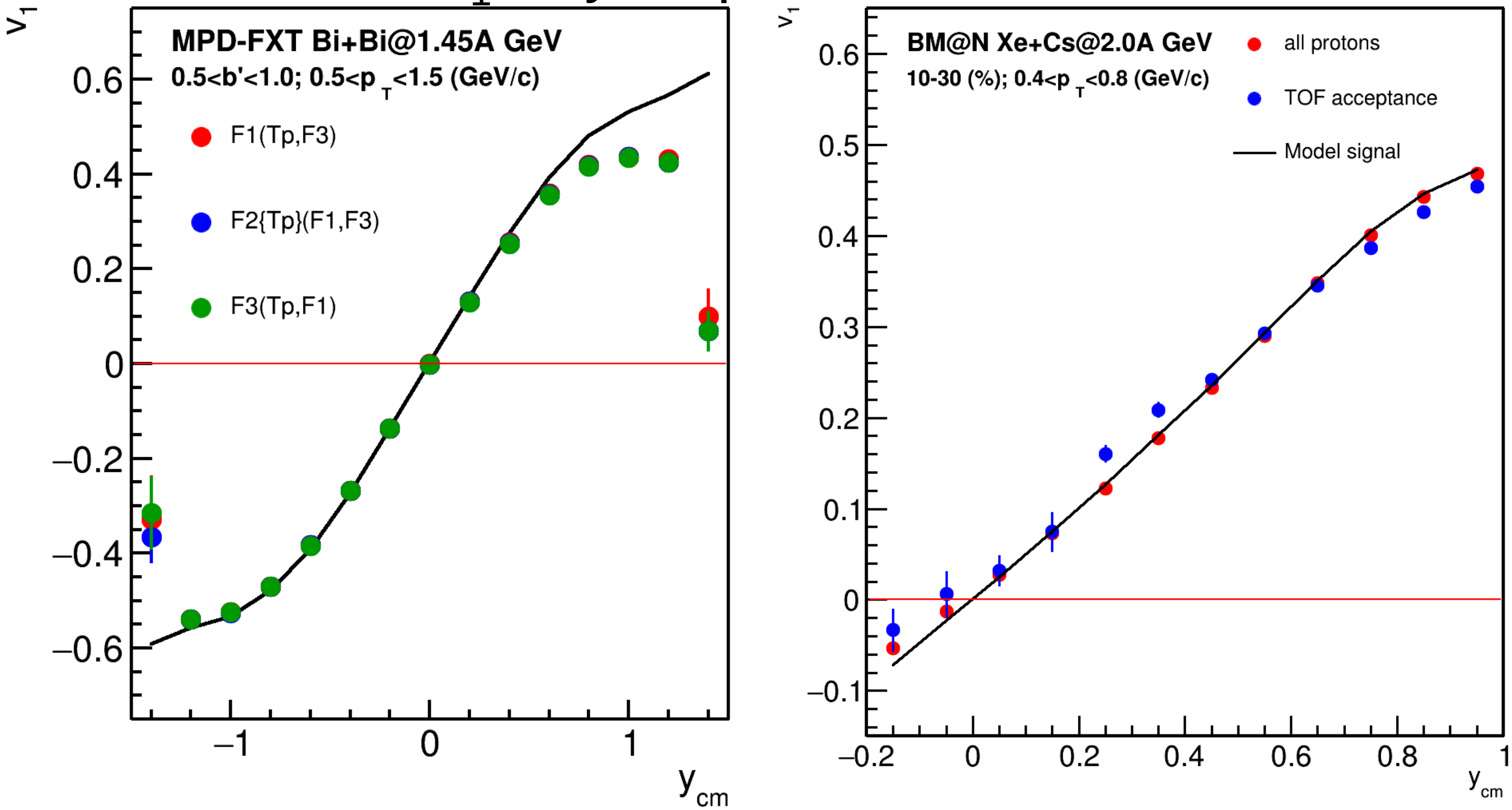

BM@N has better coverage in positive rapidities close to y_{beam}

BM@N vs MPD: v_2 vs y for protons

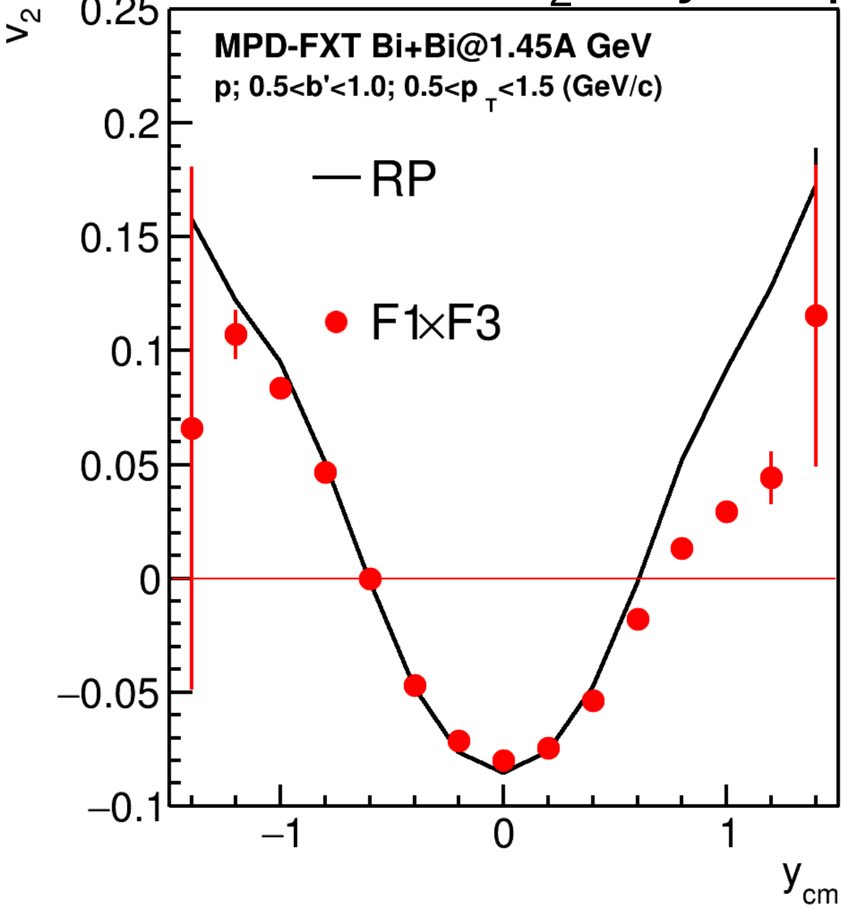

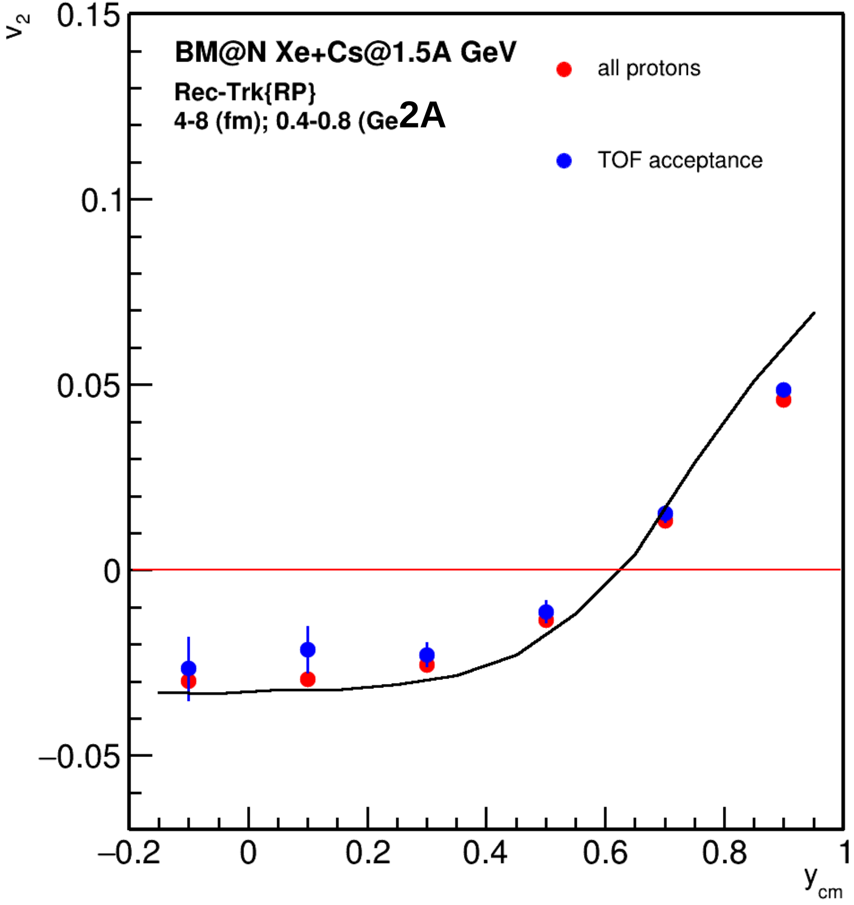

BM@N has better coverage in positive rapidities close to y_{beam}

MPD-FXT: v_1 for π+

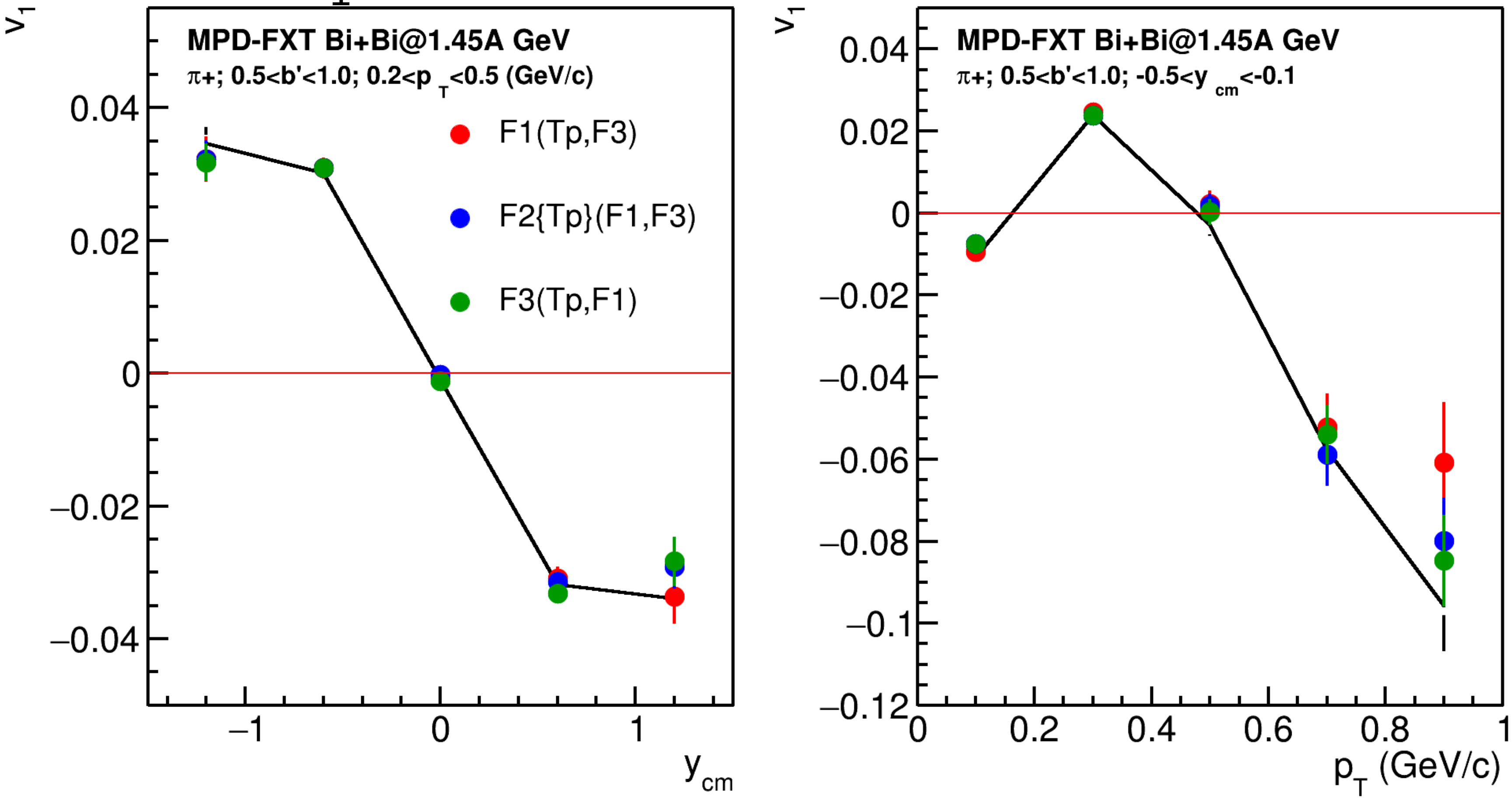

v_1 is consistent with model signal for $y < 1$; We need more statistics

MPD-FXT: v_2 for π+

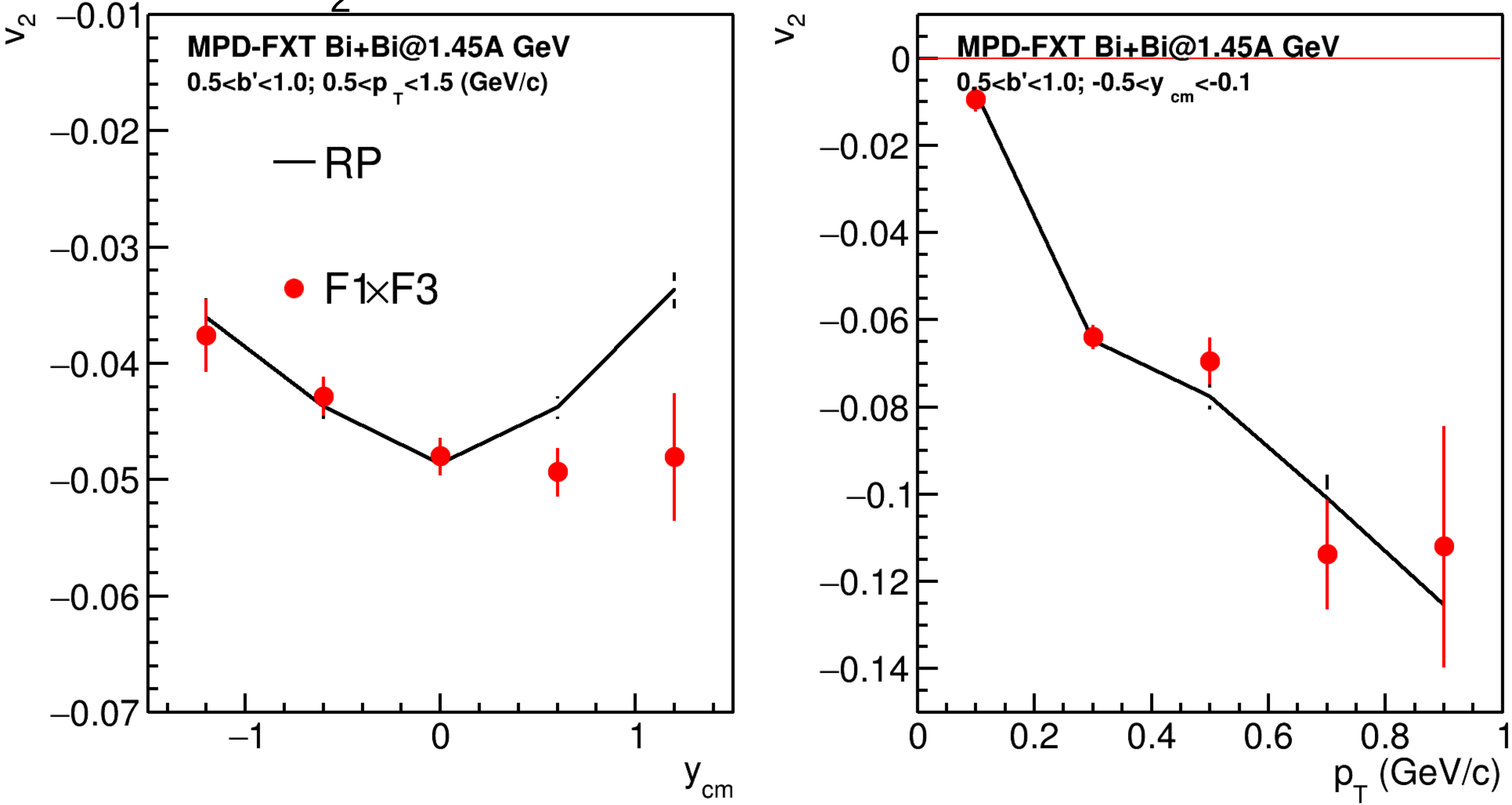

v_2 is consistent with model signal for y < 0; We need more statistics

MPD-FXT: v_1 for π-

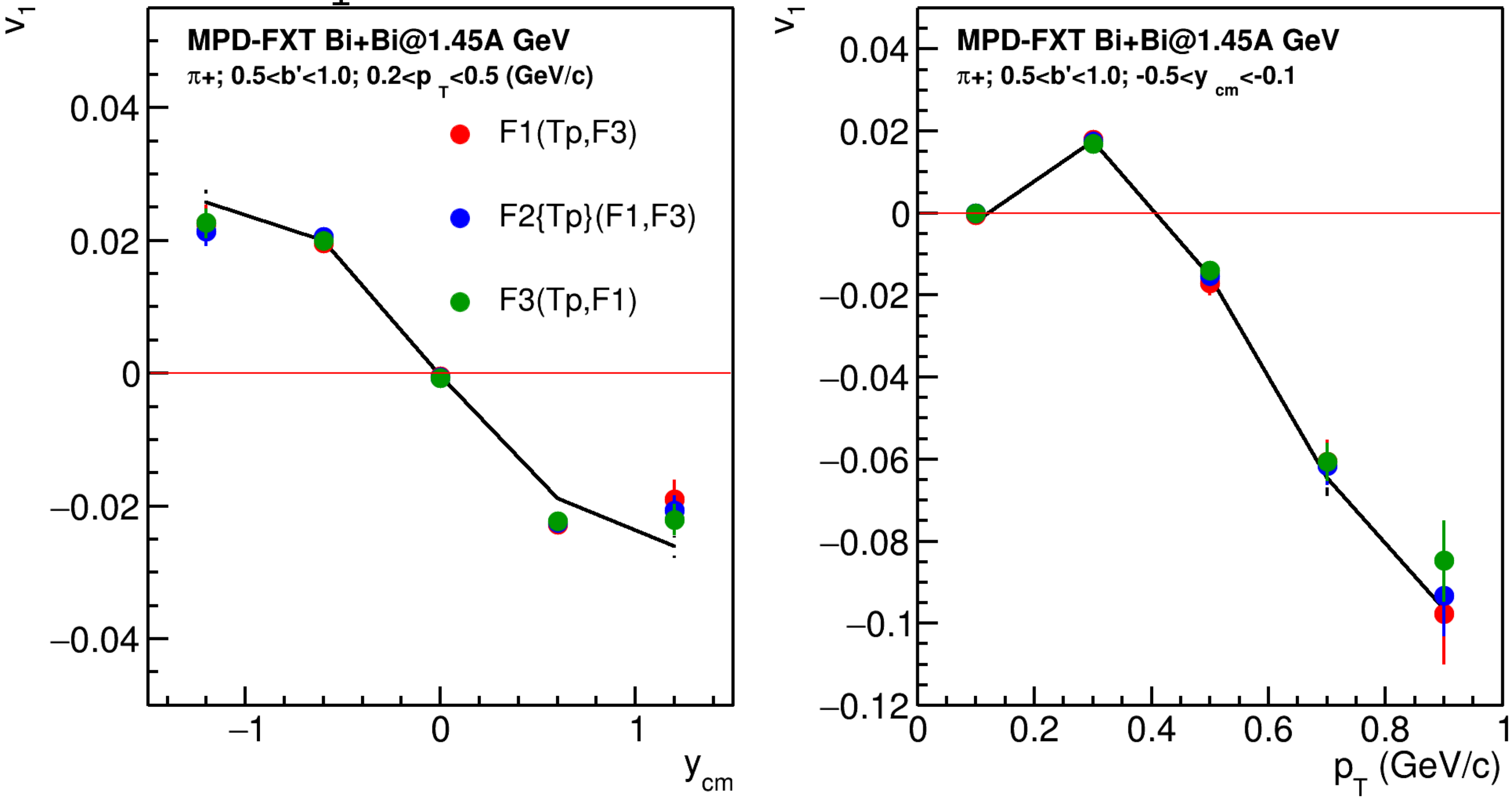

v_1 is consistent with model signal for y < 1; We need more statistics

MPD-FXT: v_2 for π-

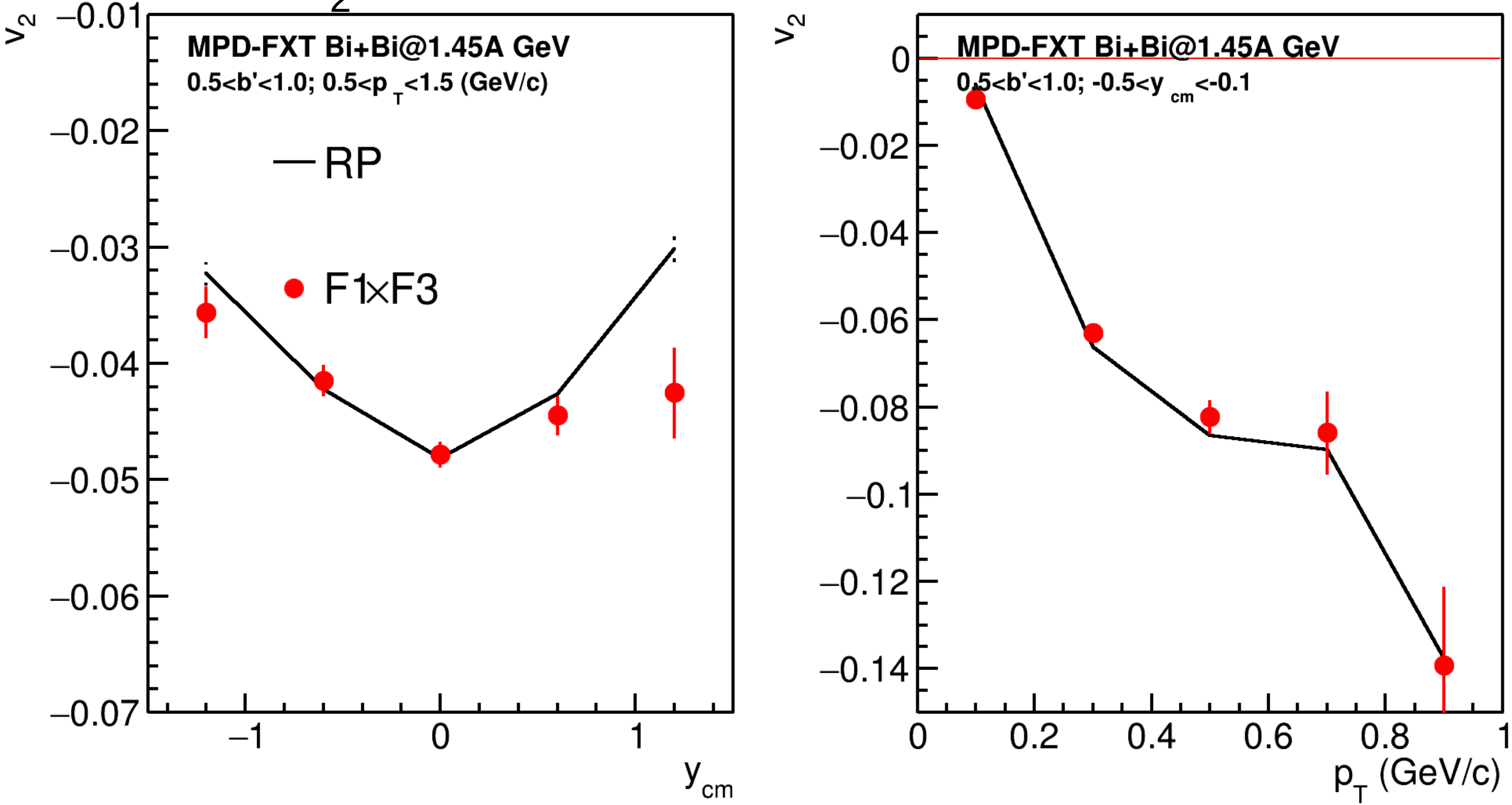

v_2 is consistent with model signal for y < 0; We need more statistics

Anisotropic transverse flow

Spatial asymmetry of energy distribution at the initial state is transformed, through the strong interaction, into momentum anisotropy of the produced particles.

$$E\frac{d^3N}{d^3p} = \frac{1}{2\pi}\frac{d^2N}{p_T dp_T dy}\left(1+\sum_{n=1}^{\infty} 2v_n\cos(n(\phi-\Psi_{RP}))\right)$$

⇓

$$v_n = \langle \cos(n(\phi - \Psi_{RP}))\rangle$$

In the experiment reaction plane angle Ψ_{RP} can be approximated by participant Ψ_{PP} or spectator Ψ_{SP} symmetry planes.

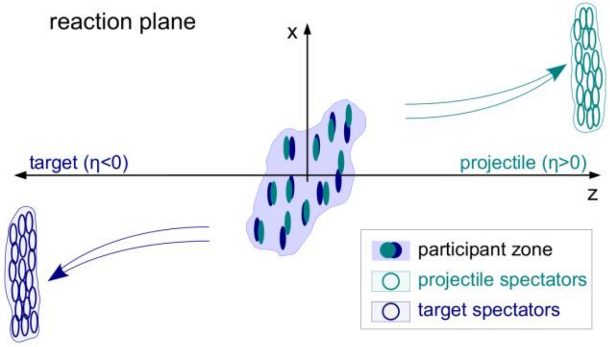

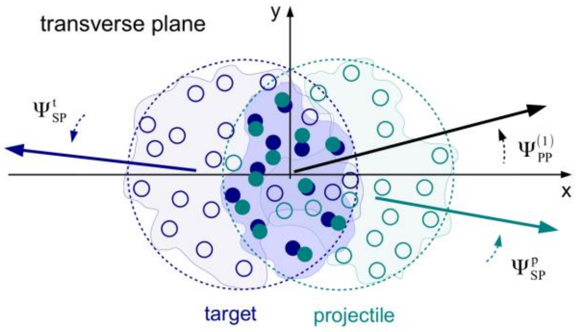

Anisotropic transverse flow in heavy-ion collisions at Nuclotron-NICA energies

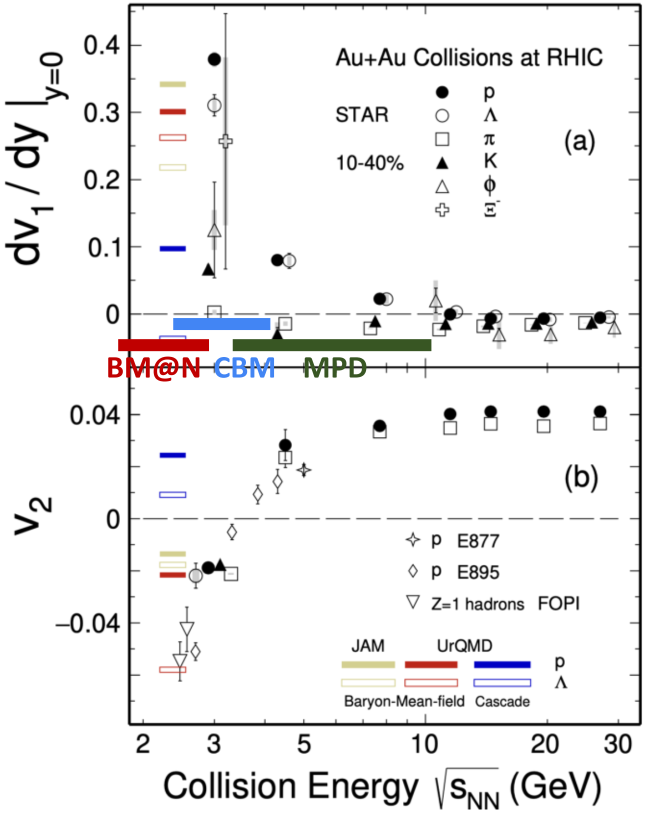

Strong energy dependence of dv_1/dy and v_2 at $\sqrt{s_{NN}}$ =4-11 GeV.

Anisotropic flow at FAIR/NICA energies is a delicate balance between:

- The ability of pressure developed early in the reaction zone and
- Long passage time (strong shadowing by spectators).

Differential flow measurements $v_n(\sqrt{s_{NN}}$, centrality, pid, p_T, y) will help to study:

- effects of collective (radial) expansion on anisotropic flow
- interaction between collision spectators and produced matter
- baryon number transport

Several experiments (MPD, BM@N, STAR FXT, CBM, HADES, NA61/SHINE) aim to study properties of the strongly-interacted matter in this energy region.

M. Abdallah et al. [STAR Collaboration] 2108.00908 [nucl-ex]